Birefringence of light in magnetically ordered crystals

G. A. Smolenskiĭ, R. V. Pisarev, and I. G. Siniĭ

A. F. Ioffe Physico-technical Institute, USSR Academy of Sciences, Leningrad
Usp. Fiz. Nauk **116**, 231–270 (June 1975)

This review is concerned with the propagation of electromagnetic waves in magnetically ordered crystals, including the subjects of circular, linear, and elliptic birefringence. New optical phenomena in crystals are analyzed on the basis of magnetic symmetry. Microscopic mechanisms of magneto-optic effects suggested so far are reviewed. Problems in crystal optics of magnetically ordered media are considered. The main results of experimental investigations of magnetic birefringence of light in ferromagnets, ferrimagnets, and antiferromagnets are discussed.

PACS numbers: 78.20.F, 78.20.L

CONTENTS

I. INTRODUCTION

About 40 years ago, the present journal (Usp. Fiz. Nauk) published a translation[1] of a review by Beams on the birefringence in electric and magnetic fields. Beams discussed the most important studies of the effects observed during the passage of light through media at right-angles to the force lines of electric and magnetic fields. He reviewed almost a century of the development of electrooptics and magnetooptics. This branch of physics was founded in 1845 by Faraday's discovery of the rotation of the plane of polarization of light during its propagation through transparent media parallel to the magnetic force lines. Single-minded investigations of Faraday, who sought a relationship between light, electricity, and magnetism, have continued to stimulate for over a century an increasingly intensive search for new phenomena in electrooptics and magnetooptics. Among the numerous examples of these phenomena, the most important are the Kerr, Zeeman, and Cotton-Mouton effects.

Beams considered mainly the Cotton-Mouton effect in liquids because detailed measurements had only been made in such media. The Cotton-Mouton effect in crystals (also known as the Voigt effect) was dismissed in few general sentences describing the work of Becquerel (see [2,3]), Becquerel investigated crystals doped with rare-earth ions and discovered, near absorption lines, a change in the polarization of light due to the Zeeman effect. One should mention here the frequent reminder in Beams' review that, in measurements of magnetic birefringence, one has to separate this effect from the always present strong magnetic circular birefringence (Faraday effect).

A radical change occurred in optical investigations of magnetically ordered crystals after the discovery of materials highly transparent over wide ranges of infrared, visible, and even ultraviolet light. However, for many years, investigations have been limited to the Faraday effect. This effect is discussed in several review papers[4-8] and we shall not deal with it in detail. We shall concentrate our attention on the magnetic linear birefringence in nonmetallic ferromagnets and antiferromagnets.

Even the first investigations demonstrated the unusual strength of the magnetic birefringence in magnetically ordered crystals.[9,10] For example, a magnetic birefringence $n_{\parallel} - n_{\perp} \approx 1.5 \times 10^{-2}$ was reported in [10] for the ferromagnet EuSe; this is still a record value for crystals.

Many studies have recently been made of the linear birefringence of substances with different types of magnetic order. Numerous aspects of this interesting phenomenon have been revealed, such as the large magnitude and anisotropy of the effect in magnetic crystals, coexistence of linear and circular birefringence, and relationship between linear birefringence and magnetization. Therefore, it has become necessary to generalize and arrange systematically the available information, which is done in the present review.

In the first chapters, we shall consider some general aspects of the propagation of light in magnetically ordered crystals and later we shall discuss the main experimental results obtained on the magnetic linear birefringence.

II. CHARACTERISTICS OF PROPAGATION OF ELECTROMAGNETIC WAVES IN MAGNETICALLY ORDERED CRYSTALS

1. **Magnetic circular and linear birefringence.** The propagation of electromagnetic waves is described by Maxwell equations[11] and the properties of the media through which such waves travel can be allowed for by introducing the permittivity ϵ_{ik} and permeability μ_{ik}. The relationships between the electric and magnetic in-

duction and the corresponding electric and magnetic fields of light waves are

$$D_i = \varepsilon_{ik}E_k, \quad B_i = \mu_{ik}H_k. \tag{1}$$

If allowance is made for the spatial dispersion or the magnetoelectric interaction, the above relationships are modified, but this point will be considered later.

Magnetooptic effects appear when a medium in which light is traveling is subjected to an external magnetic field (which may be static or may vary at a frequency lower than that of light) or when a spontaneous magnetic order exists in the medium (crystal). Since such magnetic perturbations have little effect on the optical properties of the medium, we can expand the permittivity ϵ_{ik} as a series in increasing powers of the external field or magnetization. If a crystal has a spontaneous ferromagnetic moment M, this expansion can be expressed in the form

$$\varepsilon_{ik}(\mathbf{M}) = \varepsilon_{ik}^{(0)} + f_{ikl}^{(1)}M_l + f_{iklm}^{(2)}M_lM_m + f_{iklmn}^{(3)}M_lM_mM_n + \ldots, \tag{2}$$

where $\epsilon_{ik}^{(0)}$ is the permittivity tensor of a crystal in the paramagnetic state (for which M = 0), $f_{ikl}^{(1)}$ is a third-rank tensor which governs magnetooptic effects that are linear in respect of the magnetization, $f_{iklm}^{(2)}$ is a fourth-rank tensor describing the quadratic effects, etc. A similar expansion can also be made in the case of the tensor μ_{ik}.

We shall consider the influence of terms linear in M on the nature of propagation of light in crystals. We shall assume that the magnetization is directed along one of the fourfold axes in a cubic crystal M ∥ [001]. Equation (1) can then be written in the form

$$\mathbf{D} = \begin{pmatrix} \varepsilon_{xx} & -i\varepsilon_{xy} & 0 \\ i\varepsilon_{yx} & \varepsilon_{yy} & 0 \\ 0 & 0 & \varepsilon_{zz} \end{pmatrix}\mathbf{E}, \tag{3}$$

where the antisymmetric components of the tensor are equal, $\epsilon_{xy} = \epsilon_{yx}$, and are linear functions of the magnetization. If a plane light wave travels along the magnetization, we find that

$$D_x = n^2E_x, \quad D_y = n^2E_y, \quad D_z = 0. \tag{4}$$

It follows from Eqs. (3) and (4) that, instead of one value of n^2, we have two

$$n_{\pm}^2 = \varepsilon_{xx} \pm \varepsilon_{xy}, \tag{5}$$

i.e., two waves of different velocities may travel along the direction of magnetization. The axial symmetry around the magnetication is responsible for these waves being circularly polarized with opposite rotations of the polarization vector. The superposition of these two waves produces a linearly polarized wave and the plane of polarization of this wave rotates as one circular wave overtakes the other. In the direction of propagation of the wave in a crystal, this angle of rotation is

$$\varphi_F = \frac{\pi\nu l}{c}\Delta n \cdot \cos\theta, \tag{6}$$

where ν is the frequency of light, l is the crystal length, $\Delta n = n_- - n_+ = \epsilon_{xy}/n$, θ is the angle between the magnetization and direction of propagation of light. This is known as the Faraday effect. When the magnetization is reversed, the angle of rotation of the plane of polarization changes its sign.

The formula (6) applies to those parts of the electromagnetic wave spectrum where there is no absorption. However, if absorption does occur at the wavelength under investigation, the two waves of opposite circular polarization traveling in a crystal are attenuated in different ways. This difference between the absorption coefficients of right- and left-handed circularly polarized waves is known as the magnetic circular dichroism. This phenomenon is also linear in respect of the magnetization. Since two circular waves have different amplitudes on leaving an absorbing crystal, their superposition produces light of elliptic polarization.

The Faraday effect and magnetic circular dichroism are related by the integral Kramers-Kronig relationships (see [11]). Although both these effects are used in investigations, the magnetic circular dichroism is a more direct and convenient method (in combination with optical absorption) for investigating the energy states of crystals.

It follows from Eq. (6) that, when light travels at right-angles to the magnetization, linear magnetooptic effects vanish and, in this case, we can determine the role of the magnetization by including the next term $f_{iklm}^{(2)}M_lM_m$ of the expansion (2). We shall assume that a light beam travels along the x axis of a cubic crystal magnetized along the z axis. In this geometry, we have

$$D_x = 0, \quad D_y = n^2E_y, \quad D_z = n^2E_z. \tag{7}$$

Using Eqs. (7) and (3), we find that two normal waves, polarized linearly along and at right-angles to the magnetization, may travel in a crystal:

$$n_z = \sqrt{\varepsilon_{zz}}, \quad n_y = \sqrt{\varepsilon_{yy} - \frac{\varepsilon_{xy}^2}{\varepsilon_{xx}}}. \tag{8}$$

The different phase velocities of these two waves give rise to a linear biregringence of light, known as the Cotton-Mouton or Voigt effect. In this case, the light emerging from a crystal has elliptic polarization. The degree of ellipticity depends on the difference between the refractive indices $\Delta n = n_Z - n_Y$. The phase shift produced by passing through a crystal of thickness l can be found from

$$\Delta_{CM} = \frac{2\pi\nu l}{c}\Delta n. \tag{9}$$

In the selected geometry with M ∥ [001], the x and y axes are equivalent, i.e., $\epsilon_{XX} = \epsilon_{yy}$ (cubic crystal). Using Eq. (8), we can find the difference between the refractive indices

$$\Delta n = \frac{1}{2}\left(\Delta\varepsilon + \frac{\varepsilon_{xy}^2}{\varepsilon_{yy}}\right), \tag{10}$$

where $\Delta\epsilon = \epsilon_{ZZ} - \epsilon_{yy}$. Thus, the magnetic linear birefringence depends both on the square of the nondiagonal component of the tensor ϵ_{ik}, governing the circular birefringence of light (Faraday effect), and on the difference between the diagonal components, which include corrections that are quadratic functions of the magnetization.

In the perpendicular geometry, the magnetization also gives rise to a difference between the absorption coefficients of waves with orthogonal linear polarizations, which produces the magnetic linear dichroism of crystals in the region of fundamental absorption bands.

2. Elliptic birefringence. The circular and linear birefringence effects are special cases of the birefringence of elliptically polarized waves. The elliptic birefringence is encountered in the propagation of light in

diamagnetic or paramagnetic optically active crystals along directions which do not coincide with the optic axes (for example, in quartz). The elliptic birefringence is possible also in magnetically ordered crystals whose permittivity tensor (expressed in the principal axes system) is

$$\varepsilon=\begin{pmatrix} \varepsilon_{xx} & i\varepsilon_{xy} & i\varepsilon_{xz} \\ -i\varepsilon_{yx} & \varepsilon_{yy} & i\varepsilon_{yz} \\ -i\varepsilon_{zx} & -i\varepsilon_{zy} & \varepsilon_{zz} \end{pmatrix}. \tag{11}$$

The elliptic birefringence is observed experimentally when the nondiagonal components are comparable with the difference between the diagonal components. In fact, if a crystal has a permittivity tensor of the type given by Eq. (1) and $\mu = 1$, the solution of Maxwell equations gives two wave vectors for the light traveling along the z axis:

$$k_{\pm}=\frac{\omega^2}{2}[(\varepsilon_{xx}+\varepsilon_{yy})\pm\sqrt{(\varepsilon_{yy}-\varepsilon_{xx})^2+4\varepsilon_{xy}^2}]. \tag{12}$$

The normal modes then have elliptic polarizations with the ellipse axes directed along the x and y axes:[12]

$$\begin{pmatrix} E_x' \\ E_y' \end{pmatrix}=A'\begin{pmatrix} 1 \\ -i/\alpha \end{pmatrix}\exp[i(\omega t-k_+z)],\quad \begin{pmatrix} E_x'' \\ E_y'' \end{pmatrix}=A''\begin{pmatrix} 1 \\ i\alpha \end{pmatrix}\exp[i(\omega t-k_-z)], \tag{13}$$

where A is an arbitrary amplitude and

$$\alpha=\frac{2\varepsilon_{xy}}{2\varepsilon_{xx}-[(\varepsilon_{xx}+\varepsilon_{yy})+\sqrt{(\varepsilon_{yy}-\varepsilon_{xx})^2+4\varepsilon_{xy}^2}]}. \tag{14}$$

The system (13) describes two orthogonal elliptically polarized waves. This system describes also two extreme cases in the propagation of light: if $\epsilon_{xy} = 0$, we have the usual linear birefringence and waves are propagated with a linear polarization; if $\epsilon_{xx} = \epsilon_{yy}$, only the circular birefringence is observed and waves with left- and right-handed circular polarization are propagated.

The equations for the normal modes can be transformed for the x and y components of the electric field, which makes it possible to find the relative amplitudes and phases of these components at any point z in the direction of propagation:

$$\begin{pmatrix} E_x \\ E_y \end{pmatrix}_{z=l} \tag{15}$$
$$=\begin{pmatrix} \cos(\Phi/2)-i\cos\chi\sin(\Phi/2) & -\sin\chi\sin(\Phi/2) \\ \sin\chi\sin(\Phi/2) & \cos(\Phi/2)+i\cos\chi\sin(\Phi/2) \end{pmatrix}\begin{pmatrix} E_x \\ E_y \end{pmatrix}_{z=0},$$

where $\Phi = \delta z$, $\delta = k_+ - k_-$, $\cos\chi = (1-\alpha^2)/(1+\alpha^2)$, $\sin\chi = 2\alpha/(1+\alpha^2)$. The matrix in the first set of parentheses on the right is the Jones matrix, describing the propagation of light in a medium.[13] Equation (15) gives the relative shift between the electric vectors.

We shall now consider some consequences of Eq. (15). Let us assume that a wave of unit amplitude, polarized along the x axis, is incident on a crystal. On leaving this crystal at $z = l$, we find that this wave is described by

$$(E_x)_l=\cos\frac{\Phi}{2}-i\cos\chi\cdot\sin\frac{\Phi}{2},$$
$$(E_y)_l=\sin\chi\cdot\sin\frac{\Phi}{2}. \tag{16}$$

It is immediately clear that the maximum value of E_y is equal to $\sin\chi$. If the circular birefringence is weaker than the linear effect, i.e., if $|\epsilon_{xy}| \ll |\epsilon_{xx} - \epsilon_{yy}|$, the maximum value of E_y is small compared with unity. Thus, the circular birefringence now gives rise to just a slight ellipticity at the exit from the crystal. However, if there is no linear birefringence, the amplitude E_y may be equal to unity. If both effects coexist, i.e., if $0 < \sin\chi < 1$, the plane of polarization of light in the crystal cannot rotate by 90°.

If we denote the angle of rotation of the major axis of the ellipse relative to the x axis by β and if we denote the ratio of the axes by $a/b = \tan\xi$, we find from Eq. (16) that

$$\operatorname{tg}2\beta=\frac{\sin\chi\cdot\sin\Phi}{\sin^2\chi\cdot\cos\Phi+\cos^2\chi},$$
$$\sin 2\xi=\sin 2\chi\cdot\sin^2\frac{\Phi}{2}. \tag{17}$$

If $\sin\chi \ll 1$, i.e., if the linear birefringence is much stronger than the circular effect, we have

$$\beta=\frac{1}{2}\sin\chi\cdot\sin\Phi,$$
$$\xi=\frac{1}{2}\sin 2\chi\cdot\sin^2\frac{\Phi}{2} \tag{18}$$

and we can see that neither β nor ξ can be large.

We must also consider another important feature of the coexistence of the circular and linear birefringence in a crystal.[12] If we assume that $\epsilon_{xx} = \epsilon_0 - \eta$ and $\epsilon_{yy} = \epsilon_0 + \eta$ and if we substitute these values into the equations for δ^2, we obtain

$$\delta^2=\frac{\omega^2\eta^2}{\varepsilon_0}+\frac{\omega^2\varepsilon_{xy}^2}{\varepsilon_{yy}}+O(\eta^4,\ \varepsilon_{xy}^4). \tag{19}$$

Ignoring the terms η^4 and ϵ_{xy}^4 and those of higher orders of smallness, we find that the first term in Eq. (19) gives the linear birefringence of a medium in radians per unit length in the absence of circular birefringence:

$$\rho=\sqrt{\frac{\omega^2\eta^2}{\varepsilon_0}}. \tag{20}$$

The second term gives the circular birefringence in radians per unit length in the absence of linear birefringence:

$$2\theta=\sqrt{\frac{\omega^2\varepsilon_{xy}^2}{\varepsilon_0}}. \tag{21}$$

Thus, with an accuracy to within the rejected terms, we can formulate the following principle of superposition of the linear and circular birefringence:

$$\delta=2\sqrt{\theta^2+\left(\frac{\rho}{2}\right)^2},$$
$$\cos\chi=\frac{\rho}{\delta},\quad \sin\chi=\frac{2\theta}{\delta}. \tag{22}$$

This formulation clarifies the definitions introduced above.

Apart from the work of Tabor and Chen,[12] various aspects of the propagation of light in media exhibiting circular and linear birefringence were analyzed in [14-17]. An experimental investigation of the elliptic birefringence in cubic garnet crystals, in which the circular and linear effects appear because of the magnetization, is reported in [14]. A more general expression for the Mueller matrix (see [13]) is obtained in [15] for a cubic medium exhibiting optical effects which are linear and quadratic functions of the magnetization. This expression is obtained on the basis of the principle of superposition and on the assumption that the crystal is magnetooptically isotropic.[18] It is pointed out in [15] that a crystal with elliptic birefringence may transform the state of polarization of the light flux in an unrestricted manner without additional optical elements.

The coexistence of the linear and quadratic magnetooptic effects gives rise to certain interesting features in the modulation of light when the magnetization precesses, as found, for example, in the microwave

range.[16] If light travels across a cubic crystal magnetized along the z axis, i.e., if $\mathbf{m} \parallel Oz$ and if $\mathbf{k} \parallel Oy$, the magnetization precession gives rise to components oscillating along the x and y axes:

$$m_x = \alpha m_z \cos \Omega t, \quad m_y = \alpha m_z \sin \Omega t, \tag{23}$$

where α is the amplitude coefficient and Ω the precession frequency.

If the incident light is polarized along the z axis, we find that—in the first approximation—only the electric field component along the x axis is modulated:

$$E_{xl} = -i\alpha \sin \frac{l\delta}{2} E_0 \exp\{i[(\omega+\Omega)t - kl]\}, \tag{24}$$

where $\delta = k_+ - k_-$ and $k = (k_+ - k_-)/2$. If the incident light is polarized parallel to the x axis, only the component of the electric field along the z axis is modulated. Thus, the propagation of light in a medium with an elliptic birefringence gives rise to a component which is perpendicular to the incident light. This component has a different frequency $\omega \pm \Omega$ which depends on whether the incident light is polarized relative to the static magnetization. The amplitude of the resultant component is proportional to the amplitude of the precession and varies sinusoidally with the path in a crystal l. Estimates obtained for yttrium iron garnet at $\lambda = 1.15\ \mu$, using the known components of the circular and linear birefringence ($\alpha_F = 240$ deg/cm, $\beta_{CM} = 140$–160 deg/cm) show that the first maximum of the sinusoid occurs at $l \sim 1.3$ cm.

If the incident light is polarized at 45° with respect to the direction of magnetization, an amplitude modulation is observed for both components with the precession frequency Ω.

3. Propagation of light in magnetoelectric crystals with $\epsilon \neq 1$ and $\mu \neq 1$. We have considered so far the permittivity tensor ϵ on the assumption that $\mu = 1$. The permeability is the more important tensor in the propagation of electromagnetic waves in the radiofrequency and microwave range. However, at some frequencies, the contributions of ϵ and μ may be comparable and this may give rise to new features in the propagation of electromagnetic waves.[19,20]

When ϵ and μ both differ from unity, the calculations are cumbersome even in those simple cases when both tensors ϵ and μ can be reduced simultaneously to the principal axes. Therefore, this case is considered in [19] using an invariant method which is much more convenient in the case of complex calculations. We shall not consider the details of such calculations since a whole chapter is devoted to this subject in the monograph[19] but we shall note the most important results.

In the case of transparent crystals with $\mu = 1$, there is a definite relationship between the symmetry of a crystal and the nature and number of its axes. Depending on its symmetry, a crystal may be optically biaxial, uniaxial, or isotropic. In the case of crystals with $\mu \neq 1$, the situation is different. Crystals of cubic and moderately high symmetries are still isotropic and uniaxial, respectively, but crystals of lower symmetries can be optically biaxial or uniaxial. Magnetic crystals of moderate and low symmetries can, moreover, be unirefringent. In these crystals, all three values of the tensor $\gamma = \mu^{-1}\epsilon$ are identical, i.e., the tensors ϵ and μ are proportional. They do not exhibit birefringence in spite of the anisotropy manifested by the dependence of the propagation velocity on the direction. In this case, a wave with any state of polarization or unpolarized light may travel along any direction.

The propagation of waves is considered theoretically in [20] for nonabsorbing media; it is assumed that both tensors can be reduced simultaneously to the principal axes and that not only the diagonal components but also the nondiagonal components differ from zero (i.e., the media are gyrotropic in respect of ϵ and μ).

Media exhibiting anisotropy and gyrotropy of ϵ and μ simultaneously are not yet known and the changes of their discovery are slight. Electric dipole transitions which contribute to ϵ are usually much stronger than the magnetic dipole transitions that govern μ. Such media might be obtained when the tensor ϵ is weakly anisotropic and its components differ little from unity. Moreover, it is unlikely that media will be found with unifringent properties, i.e., with similar magnetic and electric ellipsoids so that $\mu = k\epsilon$.

4. Propagation of light in magnetoelectric crystals. In magnetoelectric crystals, the general relationship between the inductions and fields should be[21]

$$\begin{aligned} D_i &= \varepsilon_{ij}(\omega, k) E_j + \alpha_{ij}(\omega, k) H_j, \\ B_i &= \beta_{ij}(\omega, k) E_j + \mu_{ij}(\omega, k) H_j, \end{aligned} \tag{25}$$

where the magnetoelectric susceptibility constants are related by (in accordance with the Onsager principle):

$$\alpha_{ij} = \beta_{ji}^*. \tag{26}$$

Special features of the propagation of light in magnetoelectric crystals are considered theoretically in [21-24]. The problem was first formulated in [22] soon after the discovery of the magnetoelectric effect.[25] It was shown in [22] that even the refractive index of a lossless medium should benerally be complex, i.e., that plane waves could not travel without attenuation. However, it was later shown[23] that an error was made in [22] and that plane waves could travel without attenuation for any value of the magnetoelectric coupling constant.

The ratio of the amplitudes of the waves traveling along the x axis is[23]

$$\begin{aligned} \frac{E_z}{E_y} &\sim \pm \frac{(\eta_y - \eta_z)\sqrt{\tilde{\varepsilon}_y \mu_z \mu_y}}{\mu_y \tilde{\varepsilon}_z - \mu_z \tilde{\varepsilon}_y}, \\ \frac{E_y}{E_z} &\sim \pm \frac{(\eta_y - \eta_z)\sqrt{\tilde{\varepsilon}_z \mu_y \mu_z}}{\mu_z \tilde{\varepsilon}_y - \mu_y \tilde{\varepsilon}_z}, \end{aligned} \tag{27}$$

where $\epsilon_i = \epsilon_{ii} - (\alpha_{ii}^2/\mu_{ii})$, $\eta_i = \alpha_{ii}^2/\mu_{ii}$. If the magnetoelectric effect is absent, i.e., if $\eta_y - \eta_z = 0$, Eq. (27) represents waves with electric vectors polarized along the y and z axes. The magnetoelectric coupling alters the propagation velocities of the waves so that the polarization is no longer oriented exactly along the y or z axis, i.e., the waves acquare an elliptic polarization.

The magnetoelectric effect is analyzed by the perturbation theory method in [21] and it is shown there that the real part of the magnetoelectric tensor alters the state of polarization of linearly polarized light as it travels along a crystal. The imaginary part of this tensor gives rise to an optical activity, i.e., to a progressive rotation of the plane of polarization. It is also shown in [21] that different methods of approach to the equations relating the inductions **D** and **B** and the fields **E** and **H**, namely, expressions such as Eqs. (25) and (28), give—in the final analysis—the same optical effects.

Crystal optics of magnetoelectric media is considered in [24] by an invariant method and the influence of

the magnetoelectric effect on the propagation of light in crystals of specific magnetic classes is discussed. The role of the magnetoelectric effect in the gyrotropic birefringence is demonstrated in [26].

Only theoretical investigations have been made of the optics of magnetoelectric media. In spite of the fact that the estimates predict a very weak influence of the magnetoelectric effect on the optical properties, experimental investigations of this effect would be of interest.

III. PRINCIPLES OF MAGNETIC SYMMETRY AND OPTICAL PHENOMENA IN CRYSTALS

Allowance for the magnetic symmetry, i.e., the symmetry which includes the operation of time inversion (or a reversal of the direction of the current), has led to the prediction and discovery of several new physical effects in magnetically ordered crystals. These effects include weak ferromagnetism,[27,28] magnetoelectric effect,[25] piezomagnetism,[11,29] and several galvanomagnetic effects.[30] All these phenomena are due to the presence of a preferential direction of antiferromagnetic order in a crystal. Allowance for the magnetic symmetry may clearly give rise to new optical phenomena in crystals.[31,32]

Allowance for the spatial dispersion, i.e., for the effects due to the existence of inhomogeneities of the electric field of a light wave over distances of the order of the atomic spacing, modifies the relationship between the electric induction and the field of a light wave so that, instead of Eq. (1), we have[11]

$$D_i = \varepsilon_{ik}E_k + \gamma_{ikl}\frac{\partial E_k}{\partial x_l}, \qquad (28)$$

where ϵ_{ik} and γ_{ikl} are functions of the frequency of light. We shall now consider the properties of the tensors ϵ_{ik} and γ_{ikl}. Following the monographs,[33] we shall divide the tensors describing physical quantities or parameters of crystals into i and c tensors, where the components of an i tensor remain invariant under time inversion, whereas the components of a c tensor change their sign as a result of such inversion.

In the absence of an external magnetic field H or spontaneous magnetic order, we can readily establish the symmetry properties of the tensors ϵ_{ik} and γ_{ikl}. A generalized symmetry principle for the transport coefficient shows that ϵ_{ik} contains only the symmetric and γ_{ikl} only the antisymmetric parts, respectively:

$$\varepsilon_{ik}^{s} = \varepsilon_{ki}^{s}, \quad \gamma_{ikl}^{a} = -\gamma_{kil}^{a}. \qquad (29)$$

The tensor γ_{ikl} has a number of special features in the case of pyroelectric nonmagnetic crystals,[34] but we shall not consider them here.

The properties of the tensors ϵ_{ik} and γ_{ikl} under coordinate and time-inversion transformations are given in Table I. The symmetric part of ϵ_{ik} describes the linear birefringence and linear dichroism effects, whereas the antisymmetric part of γ_{ikl} describes the natural optical activity and circular dichroism.

In the presence of an external magnetic field, the tensors ϵ_{ik} and γ_{ikl} have antisymmetric and symmetric parts, respectively. They are linear functions of the field

$$\varepsilon_{ik}^{a}(H) = -\varepsilon_{ki}^{a}(H), \quad \gamma_{ikl}^{s}(H) = \gamma_{kil}^{s}(H). \qquad (30)$$

It is shown in Table I that the antisymmetric part ϵ_{ik}^{a} represents an irreversible rotation of the plane of polarization of light or the Faraday effect, as well as the magnetic circular dichroism.

TABLE I. Properties of ϵ_{ik} and γ_{ikl} tensors under coordinate transformations (inversion I) and time inversion (R) operations and corresponding optical effects in crystals (plus and minus signs indicate whether the sign of the effect is invariant or changes as a result of transformation; Re and Im denote the real and imaginary parts of tensors)

Tensor	Part of tensor	I	R	Optical effect
Re ε_{ik}	Symmetric	+	+	Linear birefringence
Im ε_{ik}	Ditto	+	+	Linear dichroism
Im ε_{ik}	Antisymmetric	+	−	Nonreciprocal circular birefringence (Faraday effect)
Re ε_{ik}	Ditto	+	−	Nonreciprocal circular dichroism
Re γ_{ikl}	Ditto	−	+	Reversible circular birefringence (optical activity)
Im γ_{ikl}	Ditto	−	+	Reversible circular dichroism
Re γ_{ikl}	Symmetric	−	−	Nonreciprocal linear dichroism
Im γ_{ikl}	Ditto »	−	−	Nonreciprocal birefringence

TABLE II. Transformations of tensors governing Faraday effect (FE) and Cotton-Mouton effect (CME) in magnetically ordered crystals

Effect	Tensor	Rank	Transformation properties	Examples
Magnetic FE	α_{ikl}	3	Axial i tensor	Dia- and paramagnets in magnetic field; ferro- and ferrimagnets
Antiferromagnetic FE	β_{ikl}	3	Ditto	Ferrimagnets; crystals with weak ferromagnetism
FE in electric field	ξ_{ikl}	3	Polar i tensor	Magnetoelectric materials
FE due to elastic deformation	δ_{ikln}	4	Polar c tensor	Piezomagnetic materials
Magnetic CME	a_{ikln}	4	Ditto	Dia- and paramagnets in magnetic field; ferro- and ferrimagnets
Antiferromagnetic CME	b_{ikln}	4	Polar i tensor	Antiferromagnets; ferrimagnets
Bilinear CME	c_{ikln}	4	Tensor of type i	Crystals with weak ferromagnetism

The symmetric part represents the irreversible or gyrotropic birefringence. We shall consider the optical effects that may arise from the presence of magnetic order in a crystal and from the application of electric fields or elastic stresses to a magnetic crystal.[31] We shall describe the magnetic order by the ferromagnetic $\mathbf{m} = (\mathbf{M}_1 + \mathbf{M}_2)/2\mathbf{M}_0$ and antiferromagnetic $\mathbf{l} = (\mathbf{M}_1 - \mathbf{M}_2)/2\mathbf{M}_0$ moment vectors. We shall assume that external forces and magnetic order have relatively little influence on the optical properties. Then, the antisymmetric part of the permittivity tensor describing the Faraday effect can be written in the form

$$\varepsilon_{ik}^{a} = \alpha_{ikl}m_l + \beta_{ikl}l_l + \xi_{ikl}E_l + \delta_{ikln}\sigma_{ln}. \qquad (31)$$

Knowing the properties of the tensors ϵ_{ik}^{a}, m_l, l_l, E_l, and σ_{ln}, we can readily find the properties of the other tensors occurring in the expansion (31) and then determine the existence of a given tensor for a specific magnetic structure (Table II).

The first term on the right-hand side describes the Faraday effect which appears in the presence of a diamagnetic, paramagnetic, or ferromagnetic moment in a crystal. This effect is governed by an axial third-rank i tensor α_{ikl}. Every crystal has this tensor and the symmetry considerations simply limit the number of independent components to one for isotropic and cubic media, two for optically uniaxial media, and three for optically biaxial crystals.

We shall now analyze the possibility of the appearance of the Faraday effect due to the presence of the antiferromagnetic vector l. This effect is clearly possible if the properties of the transformation of the vector l or some of its components are identical to the

properties of the transformation of the axial vector m or its components. All the components of l may transform like the components of m only in ferrimagnets when there is no sublattice transposition operation. The Faraday effect in ferrimagnets can be regarded as the sum of the effects due to the vectors m and l, and the contribution of the latter can be found at the magnetic compensation point of the ferrimagnet because, at this point, we have m = 0.

The Faraday effect in antiferromagnets due to the vector l should also be observed for those components l_k which transform in accordance with the same irreducible representations as the components m_k. It should be noted that this admits of the existence of terms of the $m_k l_n$ type in the thermodynamic potential and this is the condition for the appearance of weak ferromagnetism in a crystal.

It follows from the expansion (31) and Table II that, in certain magnetically ordered structures, the Faraday effect may appear on the application of an electric field to a crystal. This phenomenon is due to the existence of a polar third-rank c tensor ξ_{ikl}, whose components do not vanish if a given magnetic structure does not have an inversion center. A polar third-rank tensor ξ_{ikl} is dual to an axial second-rank tensor and the latter governs the possibility of the appearance of the magnetoelectric effect in a crystal.

The magnetic symmetry may also give rise to the Faraday effect if a crystal is deformed. This case is governed by a polar fourth-rank c tensor δ_{ikln} which is antisymmetric in respect of the first pair of indices and symmetric in respect of the second pair. This tensor is accompanied by components of an axial third-rank c tensor representing the piezomagnetic effect.

Expansion of the symmetric part of the tensor ϵ^s_{ik} should contain only terms quadratic in m and l and can be represented in the form

$$\varepsilon^s_{ik} = \varepsilon^{(0)}_{ik} + a_{ikln} m_l m_n + b_{ikln} l_l l_n + c_{ikln} m_l l_n, \qquad (32)$$

where ϵ^0_{ik} is the permittivity in the paramagnetic state. The properties of the tensors in Eq. (32) are given in Table II. The birefringence governed by the polar fourth-rank i tensor a_{ikln}, which is symmetric in respect of the pairs of indices i, k and l, n, is the magnetic linear birefringence or the Cotton-Mouton effect which appears in all crystals in a magnetic field or in the presence of a spontaneous ferromagnetic moment. The tensor b_{ikln} represents the antiferromagnetic linear birefringence. Although some components of the vector l may transform differently from the components of m, which imposes restrictions on the existence of the Faraday effect, in the magnetic linear birefringence case the antiferromagnetic vector l should always give rise to an effect analogous to that produced by the vector m because the products of the components $l_l l_n$ and $m_l m_n$ transform in a similar manner.

The specific properties of magnetically ordered crystals should be manifested not only in the antiferromagnetic birefringence but also in the birefringence which is bilinear with respect to m and l and is governed by the tensor c_{ikln}. This effect should also be observed in structures for which the product $m_l l_n$ transforms in the same way as the products $m_l m_n$ or $l_l l_n$. This is possible if the properties of the transformation of some of the components of l and m are identical, i.e., if weak ferromagnetism exists in a crystal.

The bilinear effect is interesting because, in contrast to the ferromagnetic and antiferromagnetic birefringence effects, its sign should be reversed on reversal of m if l retains its direction.

The possibility of the appearance of the optical activity and gyrotropic birefringence in magnetic crystals can be analyzed similarly. This can be done by expanding the antisymmetric and symmetric parts of the tensor γ_{ikl} as a series in components m_n, l_n, E_n, and σ_{nm}. Such an analysis shows that the nonreciprocal gyrotropic birefringence effect may be observed in antiferromagnets whose structure allows the existence of the magnetoelectric effect.

The question of the existence of nonzero tensors ϵ^s_{ik}, ϵ^a_{ik}, γ^a_{ikl}, and γ^s_{ikl} is considered in [32]. However, allowance for the magnetic symmetry leaves open the question of the magnitude of the effects involved. If the magnitude is needed, it is necessary to analyze in detail the microscopic mechanisms which contribute to the polarizability of a crystal subjected to a light wave. Some of the possible mechanisms are discussed in Chap. IV.

IV. SPIN-DEPENDENT POLARIZABILITY AND MICROSCOPIC MECHANISMS OF MAGNETOOPTIC EFFECTS

The interaction of light with a crystal is governed by the polarizability of individual ions, pairs of ions, etc. The polarizability terms making the greatest contribution to the magnetooptic effects should be functions of the magnetization of individual ions and can be expressed in the form[35]

$$\alpha_j(\omega) = \sum_\mu \alpha^\mu_j(\omega) S_{j\mu} + \sum_{\mu,\nu} \alpha^{\mu\nu}_j(\omega) S_{j\mu} S_{j\nu} + \ldots, \qquad (33)$$

$$\alpha_{jl}(\omega) = \sum_{\mu,\nu} \alpha^{\mu\nu}_{jl}(\omega) S_{j\mu} S_{l\nu} + \ldots, \qquad (34)$$

where $S_{j\mu}$ is the projection of the average thermodynamic value of the spin of an ion j. The possible components of the tensors occurring on the right-hand sides of Eqs. (33) and (34) are governed by the local symmetry of the environment of individual ions and of ion pairs. The total spin-dependent polarizability of a crystal can be represented by

$$\alpha(\omega) = \sum_j \alpha_j(\omega) + \sum_{j,l} \alpha_{jl}(\omega) + \ldots, \qquad (35)$$

where the summation is carried out over all the magnetic ions and over all ion pairs, and the first and second terms on the right-hand side of Eq. (35) represent the polarizabilities of individual ions and of ion pairs, respectively.

The most general expression for the spin-dependent polarization of a pair of ions j and l is

$$\alpha^{\mu\nu}_{jl} = P^{\mu\nu}_{jl}(\mathbf{S}_j \mathbf{S}_l) + \sum_{\rho,\tau} Q^{\mu\nu}_{jl,\rho\tau} S_{j\rho} S_{l\tau} + \sum_{\rho,\tau} R^{\mu\nu}_{jl,\rho\tau} S_{j\rho} S_{l\tau}, \qquad (36)$$

where all the terms are symmetric relative to the transposition of the indices μ and ν. This form of the polarizability of an ion pair separates isotropically the exchange term proportional to P_{jl}, whereas the terms with Q_{jl} and R_{jl} are, respectively, symmetric and antisymmetric relative to the transposition of two spins or indices ρ and τ, i.e., they have the following properties:

$$Q^{\mu\nu}_{jl,\rho\tau} = Q^{\mu\nu}_{jl,\tau\rho}, \quad R^{\mu\nu}_{jl,\rho\tau} = -R^{\mu\nu}_{jl,\tau\rho}, \quad \sum_\rho Q^{\mu\nu}_{jl,\rho\rho} = 0. \qquad (37)$$

If the ion pair under consideration has an inversion center, the antisymmetric terms R_{jl} vanish. The actual

form of the tensors of pairs consisting of identical or different ions in the rutile structure is given in [35].

The interaction of light with electrons in a magnetic crystal can be described by the Hamiltonian[35-37]

$$\mathcal{H} = \mathcal{H}_{cr} + \mathcal{H}_C + \mathcal{H}_{s\text{-}o} + \mathcal{H}_Z + \mathcal{H}_{e\text{-}ph}, \qquad (38)$$

where the terms describe, respectively, the internal crystal fields, Coulomb exchange interaction of electrons, spin-orbit coupling, Zeeman energy, and interaction of electrons with photons. One-photon processes (absorption of light) can be described by the perturbation theory linear in respect to $\mathcal{H}_{e\text{-}ph}$. Moreover, the perturbation theory linear in respect of $\mathcal{H}_{e\text{-}ph}$ can describe the processes of selective absorption of polarized light (magnetic circular and linear dichroism) but we then have to include also the terms $\mathcal{H}_Z$, $\mathcal{H}_{s\text{-}o}$, $\mathcal{H}_C$. Two-photon processes (Faraday and Cotton-Mouton effects, Raman scattering) involving virtual absorption and emission of a photon with an altered polarization can be described by the theory which is quadratic in respect of $\mathcal{H}_{e\text{-}ph}$ and linear or quadratic in respect of the other terms of the Hamiltonian (38), depending on the phenomenon under discussion.

We shall not give details of the calculations reported in [35] but simply consider the results which give estimates of the polarizability coefficients a_m, p_m, etc. The third-order perturbation theory gives the following expressions for the single-ion and two-ion polarizability terms, respectively,

$$a_m \sim \frac{\theta |(g|er|a)|^2 \lambda}{\Delta E_0 \Delta E}, \qquad p_m \sim \frac{I}{\lambda} \theta^{-1} a_m. \qquad (39)$$

where $|(g)|er|a)|^2$ is the square of the moment of the electric dipole transition between ground and excited states of opposite parity, $\Delta E_0 \sim (E_a - E_g - \hbar\omega_0)$ is the energy of an odd electron excitation without allowance for the photon energy, ΔE is the energy gap between ground and the nearest level of opposite parity. I is the nondiagonal exchange integral between two ions, λ is the spin-orbit coupling constant. If the photon energy is less than ΔE, we have $\theta \sim h\omega_0/(\Delta E + 2h\omega_0)$. This parameter θ can play an important role in the case of ions of the 3d group for which the nearest odd states lie in the region of $\sim 10^5$ cm^{-1}.

We can see from the system (39) that the effects linear in respect of the magnetization (the Faraday effect in the absence of absorption) are governed by the spin-orbit interaction. This interaction is allowed for in the explanations of the Faraday effect in metals,[38-40] yttrium iron garnet $Y_3Fe_5O_{12}$,[41] and the ferromagnet $CrBr_3$.[42]

In this approximation, the quadratic magnetooptic effects depend on the nondiagonal exchange integral I.

The form of a_m and p_m in the system (39) shows that these terms may be comparable in magnitude. The contribution to the quadratic effects can also be obtained in the next approximation of the perturbation theory, namely, by double allowance for the electron-photon and spin-orbit interactions. This approximation yields the contributions A_m and A'_m to the polarizability terms:

$$A_m \sim A'_m \sim \frac{\lambda}{\Delta E} a_m \theta^{-1}. \qquad (40)$$

The double term $\mathcal{H}_C$ contributes to the biquadratic polarizability of an ion pair and the order of magnitude of this contribution is $\sim (I/\Delta E)\, p_m$. The terms which are bilinear in respect of $\mathcal{H}_{s\text{-}o}$ and $\mathcal{H}_C$ contribute to the antisymmetric polarizability terms R_{jl}; the order of magnitude of these terms is $\sim (\lambda/\Delta E)\, p_m$. Higher approximations of the perturbation theory will also make contributions which depend on $\lambda/\Delta E$ and $I/\Delta E$, but the magnitude of these contributions clearly decreases rapidly with increasing order of the approximation because, in the case of the 3d ions, we have $\lambda/\Delta E \sim I/\Delta E \sim 10^{-3}$.

V. CRYSTAL OPTICS OF MAGNETICALLY ORDERED MEDIA

1. **Gyration surfaces.** By analogy with the surfaces representing the natural optical activity along different crystallographic directions, we can introduce the concept of a gyration surface representing the magnetic rotation of the plane of polarization of light. This rotation, described by the term in the expansion (31) which is linear in respect of the magnetization, can be represented by a surface which is a linear function of the direction cosines γ_i of the radius vector r relative to the magnetization:

$$\varphi(\mathbf{r}) = M(a_1|\gamma_1| + a_2|\gamma_2| + a_3|\gamma_3|). \qquad (41)$$

where the coefficients a_i describe the specific rotation of the plane of polarization of light traveling along the magnetization directed along a selected axis. In the case of crystals of lower symmetry, we have $a_1 \neq a_2 \neq a_3$, whereas, for crystals of moderate symmetry, we have $a_1 = a_2 \neq a_3$, and for cubic crystals we find that $a_1 = a_2 = a_3$. In contrast to the gyration surfaces describing the optical activity, which are linked to the crystal axes, the magnetic gyration surfaces are linked to the magnetization.

Figure 1 shows the gyration surface of a cubic crystal when the magnetization is oriented along the x_3 axis. The radius vector drawn from the origin to the point of intersection with the surface represents the specific rotation of the plane of polarization along this direction. The symmetry group of the surface is ∞/m. If we change the direction of magnetization, the gyration surface is displaced but its size and symmetry remain constant.

When the magnetization of optically uniaxial and biaxial crystals is rotated, the gyration surface of such crystals follows the rotation of the magnetization but the dimensions of these surfaces then change in accordance with Eq. (41).

2. **Optical indicatrix of cubic magnetic crystals.** The

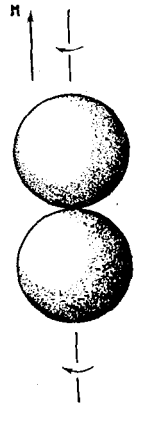

FIG. 1. Gyration surface of a cubic crystal oriented along the magnetization. The length of the radius vector drawn from the coordinate origin is proportional to the Faraday rotation of light traveling along the direction of this vector. Reversal of the direction of the propagation of light reverses the sign of rotation.

optical indicatrix describes the propagation of linearly polarized light in crystals, i.e., it describes the linear birefringence effect. In an arbitrary coordinate system, the equation for the indicatrix can be expressed in the form

$$B_{ij}x_ix_j = 1, \tag{42}$$

where i, j = 1, 2, 3; $B_{ij} = \partial E_i/\partial D_j$ are the reciprocals of the permittivity.

In the principal system of coordinates, Eq. (42) can be rewritten in the extended form

$$B_1x_1^2 + B_2x_2^2 + B_3x_3^2 = 1. \tag{43}$$

We shall now consider the influence of the quadratic term in the expansion (32) on the optical indicatrix.[18] Slight changes in the reciprocals of the permittivity, caused by the spontaneous magnetic ordering, alter the shape, dimensions, and orientation of the indicatrix. These changes can be described by specifying small changes in the coefficients B_{ij}:

$$\Delta B_{ij} = \rho_{ijkl}M_kM_l = \rho_{ijkl}\alpha_k\alpha_lM^2. \tag{44}$$

where ρ_{ijkl} is the fourth-rank magnetooptic tensor symmetric in respect of pairs of indices, and $\alpha_{k,l}$ are the direction cosines of the magnetization. For an arbitrary orientation of the magnetization, the equation for the indicatrix becomes

$$B_1x_1^2 + B_2x_2^2 + B_3x_3^2 + 2B_4x_2x_3 + 2B_5x_3x_1 + 2B_6x_1x_2 = 1. \tag{45}$$

where the system for contraction of indices is used. Equation (45) can be reduced in the usual way to the canonical form and the matrices for the transformation of the old system of the principal axes to the new can be obtained.

We shall first consider the deformation of the optical indicatrix of cubic crystals under the influence of the magnetization. Bearing in mind that the symmetric tensor ρ_{ijkl} of cubic crystals has only three independent nonzero components, which are $\rho_{1111} = \rho_{11}$, $\rho_{1122} = \rho_{12}$, and $\rho_{2323} = \rho_{44}$,[43] we can rewrite the matrix equation (44) in the extended form

$$\begin{pmatrix} \Delta B_1 \\ \Delta B_2 \\ \Delta B_3 \\ \Delta B_4 \\ \Delta B_5 \\ \Delta B_6 \end{pmatrix} = \begin{pmatrix} B_1 - B_0 \\ B_2 - B_0 \\ B_3 - B_0 \\ B_4 \\ B_5 \\ B_6 \end{pmatrix} = \begin{pmatrix} \rho_{11} & \rho_{12} & \rho_{12} & 0 & 0 & 0 \\ \rho_{12} & \rho_{11} & \rho_{12} & 0 & 0 & 0 \\ \rho_{12} & \rho_{12} & \rho_{11} & 0 & 0 & 0 \\ 0 & 0 & 0 & \rho_{44} & 0 & 0 \\ 0 & 0 & 0 & 0 & \rho_{44} & 0 \\ 0 & 0 & 0 & 0 & 0 & \rho_{44} \end{pmatrix} \begin{pmatrix} \alpha_1^2 \\ \alpha_2^2 \\ \alpha_3^2 \\ \alpha_2\alpha_3 \\ \alpha_3\alpha_1 \\ \alpha_1\alpha_2 \end{pmatrix} M^2 = \begin{pmatrix} \rho_{11}\alpha_1^2 + \rho_{12}\alpha_2^2 + \rho_{12}\alpha_3^2 \\ \rho_{12}\alpha_1^2 + \rho_{11}\alpha_2^2 + \rho_{12}\alpha_3^2 \\ \rho_{12}\alpha_1^2 + \rho_{12}\alpha_2^2 + \rho_{11}\alpha_3^2 \\ \rho_{44}\alpha_2\alpha_3 \\ \rho_{44}\alpha_3\alpha_1 \\ \rho_{44}\alpha_1\alpha_2 \end{pmatrix} M^2. \tag{46}$$

In general, Eq. (46), where the coefficients B_i can be determined from Eq. (44), describes the indicatrix of an optically biaxial crystal. For an arbitrary orientation of the magnetization, the shape of the indicatrix and its orientation are governed by the actual relationships between the magnetooptic coefficients ρ_{11}, ρ_{12}, and ρ_{44}. We shall illustrate this by considering several basic orientations of the magnetization in a cubic crystal.

1) $\mathbf{M} \parallel [001]$. For this orientation of the magnetization, we find that $\alpha_1 = \alpha_2 = 0$ and $\alpha_3 = 1$, and we can use Eq. (46) to find the changes in the principal refractive indices of the deformed indicatrix:

$$\Delta n_\parallel = \Delta n_{001} = -\frac{1}{2}n_0^3\rho_{11}M^2, \tag{47}$$

$$\Delta n_\perp = \Delta n_{100} = \Delta n_{010} = -\frac{1}{2}n_0^3\rho_{12}M^2.$$

Hence, it follows that the birefringence of a beam traveling along the [100] or [010] direction or along any other direction perpendicular to the magnetization is described by

$$\Delta n = n_\parallel - n_\perp = \frac{1}{2}n_0^3(\rho_{11} - \rho_{12})M^2. \tag{48}$$

We can see that, in this case, the magnetization converts a cubic crystal from an optically isotropic material to a uniaxial one. The indicatrix is an ellipsoid of revolution whose optic axis coincides with the direction of magnetization. The birefringence depends on the difference $\rho_{11} - \rho_{12}$ between two values of the magnetooptic tensor.

2) $\mathbf{M} \parallel [111]$. For this orientation, we have $\alpha_1 = \alpha_2 = \alpha_3 = 1/\sqrt{3}$ and Eq. (46) can be used to find the changes in the refractive indices along the direction of magnetization Δn_{111} and along any other direction perpendicular to [111], for example, Δn_{011}:

$$\begin{aligned} \Delta n_\parallel &= \Delta n_{111} = -\frac{1}{6}n_0^3(\rho_{11} + 2\rho_{12} + 2\rho_{44})M^2, \\ \Delta n_\perp &= \Delta n_{011} = -\frac{1}{6}n_0^3(\rho_{11} + 2\rho_{12} - \rho_{44})M^2. \end{aligned} \tag{49}$$

The birefringence of light traveling at right-angles to the [111] axis is

$$\Delta n = n_\parallel - n_\perp = -\frac{1}{2}n_0^3\rho_{44}M^2. \tag{50}$$

In this case, a cubic crystal is again converted from optically isotropic to uniaxial and the optic axis is oriented along the magnetization. The birefringence depends on just one component ρ_{44} of the magnetooptic tensor.

When the magnetization is oriented along other directions in a crystal, the birefringence is governed by all three components ρ_{11}, ρ_{12}, and ρ_{44} of the magnetooptic tensor and a crystal is converted from isotropic to optically biaxial. The optical behavior of cubic crystals can be described conveniently by introducing, instead of the three values of the magnetooptic tensor, a ratio of the type

$$a = \frac{\rho_{44}}{\rho_{11} - \rho_{12}}, \tag{51}$$

which describes the magnetooptic anisotropy. If a = 1, we can easily show that for any orientation of the magnetization the birefringence has the same value, i.e., it is isotropic. Moreover, in this special case, a crystal is converted to the optically uniaxial form with the axis directed along the magnetization. If $a \neq 1$, the magnetic birefringence is anisotropic and a crystal is optically biaxial. The orientations of the optic axes are governed by the parameter a. We shall now consider various possible directions of the optic axes on the assumption that the magnetization is oriented along the twofold axis: $\mathbf{M} \parallel [110]$ (Fig. 2). We can distinguish the following cases which differ in respect of the values of the magnetooptic anisotropy a.

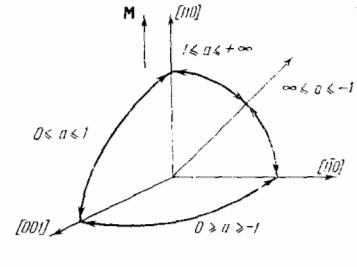

FIG. 2. Dependences of the orientations of the optic axes in a cubic cyrstal on the magnetooptic anisotropy parameter for the magnetization oriented along a two-fold axis.

a) $1 \leq |a| \leq \infty$. We shall assume that $0 \leq (\rho_{11} - \rho_{12}) \leq \rho_{44}$ and then find $n_g = n_{110}$, $n_m = n_{001}$, and $n_p = n_{110}$, where n_g, n_m, and n_p are the largest, intermediate, and smallest principal refractive indices. Using the general form for the tangent of the angle between the optic axes, we find that

$$\pm \operatorname{tg} V = \sqrt{\frac{n_m - n_p}{n_g - n_m}} = \sqrt{\frac{a-1}{a+1}}. \quad (52)$$

By definition, the optic axes lie in the plane of the indicatrix with the ellipse semiaxes n_g and n_p, i.e., the angle V is measured in this case from the (001) plane. If $a = +1$, the optic axis is directed along the magnetization, but, if $a = -1$, it is perpendicular to the magnetization and oriented along $[1\bar{1}0]$. If $a = \pm\infty$, the optic axes make an angle of 90°, i.e., they lie along mutually perpendicular fourfold axes [100] and [010]. It is interesting to note that the birefringence of magnetooptically anisotropic crystals should also be observed for the propagation of light along the magnetization (i.e., in the Faraday effect geometry) or, conversely, it may be absent for light traveling at right-angles to the magnetization.

b) $0 \leq a \leq 1$. For these values of the magnetooptic anisotropy parameter, the orientations of the optic axes can be found from

$$\pm \operatorname{tg} V = \sqrt{\frac{1-a}{2a}}, \quad (53)$$

where the angle is measured from the direction of magnetization in the $[1\bar{1}0]$ plane. If $a = 0$, the optic axis is oriented along [001] perpendicular to the magnetization.

c) $0 \geq a \geq -1$. When this condition is satisfied, the optic axes lie in the (110) plane and the angle between the optic axis and the $[1\bar{1}0]$ direction can be found from the formula

$$\pm \operatorname{tg} V = \sqrt{\frac{-1-a}{2a}}. \quad (54)$$

If $a = -1$, the optic axis coincides with $[1\bar{1}0]$.

If the magnetization is directed arbitrarily and $a \neq 1$, we can show that the optic axes are asymmetric relative to the magnetization and that this asymmetry increases with a. Consequently, in this case, none of the principal values of the refractive index coincide with the direction of magnetization. In general, the position of the indicatrix relative to the magnetization is a complex function of the value of a and of the direction cosines.

3. Optical indicatrix of uniaxial crystals. We shall now consider the influence of magnetic order on the optical indicatrix of uniaxial crystals. This problem is solved in [44,45] for cobalt carbonate $CoCO_3$ and manganese carbonate $MnCO_3$ crystals belonging to the D_{3d} class of the trigonal symmetry system. Since below the Néel point T_N these crystals have a weak ferromagnetic moment, the quadratic corrections to the coefficients B_{ij} of the optical indicatrix have the following general form[31]

$$\Delta B_{ij} = a_{ijkl} m_k m_l + \beta_{ijkl} l_k l_l + c_{ijkl} m_k l_l, \quad (55)$$

where **m** and **l** are the ferromagnetic and antiferromagnetic vectors, respectively. Bearing in mind the smallness of the spontaneous ferromagnetic moment **m**, we can ignore the contributions associated with this moment. The polar fourth-rank i tensor β_{ijkl} is symmetric with respect to index pairs and describes the primary magnetic birefringence term as well as the secondary effect due to deformation of the crystal lattice as a result of magnetic ordering. It also includes the same nonzero coefficients as the photoelastic tensor.[43] In the case of trigonal crystals of the D_{3d} class, the extended equation for the corrections to the indicatrix coefficients expressed in the form with contracted indices is[44]

$$\frac{\Delta B_m}{l^2} = \begin{pmatrix} \beta_{11} & \beta_{12} & \beta_{13} & \beta_{14} & 0 & 0 \\ \beta_{12} & \beta_{11} & \beta_{13} & -\beta_{14} & 0 & 0 \\ \beta_{31} & \beta_{31} & \beta_{33} & 0 & 0 & 0 \\ \beta_{41} & -\beta_{41} & 0 & \beta_{44} & 0 & 0 \\ 0 & 0 & 0 & 0 & \beta_{44} & 2\beta_{41} \\ 0 & 0 & 0 & 0 & \beta_{14} & \beta_{11}-\beta_{12} \end{pmatrix} \begin{pmatrix} \alpha_1^2 \\ \alpha_2^2 \\ \alpha_3^2 \\ \alpha_2\alpha_3 \\ \alpha_3\alpha_1 \\ \alpha_1\alpha_2 \end{pmatrix}; \quad (56)$$

here, α_i are the direction cosines of the antiferromagnetic vector $\mathbf{l} = (\mathbf{M}_1 - \mathbf{M}_2)/2M_0$ (there are two magnetic atoms in one unit cell of cobalt carbonate), and the coordinate system is selected in the usual manner ($Oz \parallel c_3$, $Ox \parallel u_2$).

In general, for an arbitrary orientation of the vector **l**, the nondiagonal coefficients in the equation for the optical indicatrix do not vanish, i.e., the principal axes of the indicatrix in a magnetically ordered state do not coincide with the axes of the indicatrix in the paramagnetic state. Approximate expressions of the angle of rotation of the indicatrix are obtained in [44], making allowance for the fact that the magnetic birefringence $\Delta n_m \sim 10^{-4}$ is much less than the natural crystallographic birefringence $n_o - n_e = 2 \times 10^{-1}$. An assumption that the components of the tensor β_{ik} are comparable in magnitude shows that the angles of rotation of the indicatrix are almost two orders of magnitude smaller than the angle between the optic axes in a magnetically ordered state.

If we determine the principal refractive indices confining ourselves to terms of the first order of smallness, we can ignore the deviation of the direction of n_3 from the threefold axis c_3 and we can assume that n_1 and n_2 lie in the basal plane. In this approximation, the expressions for the principal coefficients of the indicatrix become

$$B_{1,2}^{(0)} = \frac{1}{\varepsilon_{1,2}^{(0)}} = B_0 + \left\{ \frac{1}{2}(\beta_{11}+\beta_{12})(\alpha_1^2+\alpha_2^2) + \beta_{13}\alpha_3^2 \mp \left[\frac{1}{4}(\beta_{11}-\beta_{12})^2(\alpha_1^2+\alpha_2^2) + \beta_{14}^2\alpha_3^2(\alpha_1^2+\alpha_2^2) + \beta_{14}(\beta_{11}-\beta_{12})\alpha_1\alpha_3(3\alpha_1^2-\alpha_2^2) \right]^{1/2} \right\} l^2, \quad (57)$$

$$B_3^{(0)} = \frac{1}{\varepsilon_3^0} = B_e + [\beta_{31}(\alpha_1^2+\alpha_2^2) + \beta_{33}\alpha_3^2]\, l^2.$$

These expressions simplify considerably if **l** lies in the basal plane. In this case, the principal refractive indices are

$$n_1 = n_0 - \frac{1}{2}n_0^3\beta_{12}l^2, \quad n_2 = n_0 - \frac{1}{2}n_0^3\beta_{11}l^2, \quad n_3 = n_e - \frac{1}{2}n_e^3\beta_{31}l^2. \quad (58)$$

One of the principal planes of the indicatrix then passes through the antiferromagnetic vector. For light traveling along the principal directions of the indicatrix, the birefringence is

$$\left.\begin{aligned} n_1 - n_2 &= \tfrac{1}{2}n_0^3(\beta_{11}-\beta_{12})l^2 && \text{for } \mathbf{k} \parallel n_3 \ (\mathbf{k} \parallel c_3, \perp \mathbf{l}), \\ n_2 - n_3 &= (n_0 - n_e) - \tfrac{1}{2}n_0^3\left(\beta_{11} - \frac{n_e^3\beta_{31}}{n_0^3}\right)l^2 && \text{for } \mathbf{k} \parallel n_1 \ (\mathbf{k} \perp c_3, \parallel \mathbf{l}), \\ n_1 - n_3 &= (n_0 - n_e) - \tfrac{1}{2}n_0^3\left(\beta_{12} - \frac{n_e^3\beta_{31}}{n_0^3}\right)l^2 && \text{for } \mathbf{k} \parallel n_2 \ (\mathbf{k} \perp c_3, \perp \mathbf{l}). \end{aligned}\right\} \quad (59)$$

When light travels parallel to the trigonal axis, the birefringence should be independent of the orientation of the antiferromagnetic vector in the basal plane. However, if the vector **l** does not lie in the basal plane, the difference $n_1 - n_2$ depends on the orientation of the pro-

jection $l_\perp$ in the basal plane. The anisotropy of the birefringence observed on rotation of $l_\perp$ about the c_3 axis is governed by the ratio $2\alpha_3\beta_{14}/(\beta_{11}-\beta_{12})$. For small angles of the deviation of l from the basal plane (α_3 is small), the birefringence is

$$n_1-n_2=\frac{1}{2}n_0^3(\beta_{11}-\beta_{12})\left[1+\frac{2\beta_{14}}{\beta_{11}-\beta_{12}}\alpha_2\alpha_3(3\alpha_1-\alpha_2^2)\right]l^2. \quad (60)$$

Knowing the difference between the principal refractive indices, we can now determine the angle between the optic axes 2V. This angle is proportional to $\sqrt{n_g-n_m}$ and it depends linearly on the antiferromagnetic vector. If $\mathbf{l}\perp c_3$, this angle is approximately equal to

$$2V=2\sqrt{\frac{n_e^2|n_1-n_2|}{n_0|n_0^2-n_e^2|}}=2n_0n_e\sqrt{\frac{|\beta_{11}-\beta_{12}|}{2(n_0^2-n_e^2)}}\,l. \quad (61)$$

If $(\beta_{11}-\beta_{12})>0$, we find that $n_g=n_1$, $n_m=n_2$, and the optic axes lie in a plane parallel to the vector l, whereas, if $(\beta_{11}-\beta_{12})<0$, they lie in a plane perpendicular to l.

A phenomenological analysis of the influence of antiferromagnetic order on the optical properties of crystals with the tetragonal rutile structure is givenin [46]. The expression for the density of the internal electromagnetic energy in antiferromagnetic fluorides (space group D_{4h}^{14}(, including terms which are quadratic in respect of the components of the antiferromagnetic vector, is obtained in the form

$$\begin{aligned}\mathcal{E}=\mathcal{E}_0+\frac{1}{8\pi}\Big[&\lambda_1E_z^2l^2+\lambda_2(E_x^2+E_y^2)l^2+\lambda_3E_z^2l_z^2+\lambda_4(E_x^2+E_y^2)l_z^2\\&+\lambda_5E_zl_z(E_xl_x+E_yl_y)+\lambda_6E_zl_z(E_xl_y+E_yl_x)+\lambda_7E_xE_yl_xl_y\\&+\lambda_8(E_x^2-E_y^2)(l_x^2-l_y^2)\Big].\end{aligned} \quad (62)$$

As usual, the z axis is directed along the fourfold axis and the x and y axes coincide with the twofold axes, $\mathbf{l}=(\mathbf{M}_1-\mathbf{M}_2)/2M_0$ is the antiferromagnetic vector, $E_{x,y,z}$ are the components of the electric field of the incident waves, λ_k are the magnetooptic coefficients. Equation (62) is derived on the assumption that the birefringence depends primarily on the antiferromagnetic vector since the magnetization vector $\mathbf{m}=(\mathbf{M}_1+\mathbf{M}_2)/2M_0$ is two or three orders of magnitude smaller than the value of l.

The components of the symmetric permittivity tensor ϵ_{ik} can be obtained from Eq. (62) by differentiating with respect to E_i and E_k. An analysis of these components gives an interesting result: allowance for just the isotropic exchange terms makes a crystal retain its optically uniaxial properties in the magnetically ordered (antiferromagnetic) state. The resultant magnetic birefringence is proportional to the square of the antiferromagnetic vector

$$\Delta n_{\text{mag}}^{\text{isotr}}=l^2\left(\frac{\lambda_1}{n_\parallel^{(0)}}-\frac{\lambda_2}{n_\perp^{(0)}}\right), \quad (63)$$

where $n_\parallel^{(0)}=\sqrt{\epsilon_\parallel^{(0)}}$ and $n_\perp^{(0)}=\sqrt{\epsilon_\perp^{(0)}}$, i.e., the magnetic birefringence of such a crystal is independent of the direction of the vector l relative to the crystallographic axis, i.e., it is independent of the magnetic structure.

The terms anisotropic in respect of the vector components l also fail to impart biaxial properties to such a crystal when the vector l is oriented along the [001] axis ($l_x=l_y=0$, $l_z=l$). In this case the magnetic birefringence is

$$\Delta n_{\text{mag}}=l^2\left(\frac{\lambda_1+\lambda_3}{n_\parallel^{(0)}}-\frac{\lambda_2+\lambda_4}{n_\perp^{(0)}}\right). \quad (64)$$

For different orientations of the vector l at an angle with respect to the z axis, other terms of the tensor ϵ_{ik} contribute to the birefringence. The appearance of the l_x component alters the birefringence in the (z, y) plane:

$$\Delta n_{\text{mag}}^{\text{total}}=n_y-n_z=l^2\left(\frac{\lambda_1}{n_\parallel^{(0)}}-\frac{\lambda_2}{n_\perp^{(0)}}\right)+l_z^2\left(\frac{\lambda_3}{n_\parallel^{(0)}}-\frac{\lambda_4}{n_\perp^{(0)}}\right)+l_x^2\frac{\lambda_8}{n_\perp^{(0)}}. \quad (65)$$

When light travels along the z axis and $l=l_x$, the birefringence is

$$\Delta n_{\text{mag}}=n_x-n_y=\frac{2\lambda_8l_x^2}{n_\perp^{(0)}}, \quad (66)$$

i.e., it is governed only by the anisotropic terms.

As shown in the preceding chapter, the magnetic birefringence of cubic crystals alters considerably the optical properties of such crystals which usually become biaxial and the optical indicatrix can be oriented arbitrarily, depending on the orientation of the magnetization and the magnetooptic anisotropy parameter. A different situation is encountered in crystals which are uniaxial in the paramagnetic region. The magnetic birefringence of such crystals is a small perturbation compared with the crystallographic birefringence: $\Delta n_{\text{mag}}/\Delta n_{\text{cryst}}=10^{-3}-10^{-4}/10^{-1}-10^{-2}\approx 10^{-1}-10^{-3}$; rotation of the optical indicatrix is slight, of the order of several degrees.

4. Deformation of optical indicatrix due to elastic stresses and magnetostriction. The optical indicatrix may change when a crystal is deformed. This piezooptic effect can be described on the assumption that the changes in the coefficients B_{ij} of the optical indicatrix[42] are proportional to the stresses acting in a crystal:

$$\Delta B_{ij}^{\text{po}}=\pi_{ijkl}\sigma_{kl}, \quad (67)$$

where π_{ijkl} is the fourth-rank piezooptic tensor. This tensor has the same nonzero components as the fourth-rank magnetooptic tensor ρ_{ijkl} in Eq. (44). Thus, in the case of cubic crystals, the birefringence is governed by just two combinations of the piezooptic coefficients: $(\pi_{11}-\pi_{12})$ and π_{44}. Magnetically ordered crystals can become deformed not only because of the application of external stresses but also because of magnetostriction. Magnetostrictive strains ϵ_{ij}^{ms} are defined in terms of the direction cosines $\alpha_{k,l}$ of the magnetization

$$\epsilon_{ij}^{ms}=\lambda_{ijkl}\alpha_k\alpha_l. \quad (68)$$

Thus, in general, the birefringence observed in a magnetically ordered crystal may be due to the "intrinsic" magnetic birefringence or "secondary" effect because of magnetostrictive strains. Although both these effects are functions of magnetization, their microscopic nature should be different. The intrinsic magnetic birefringence is due to the splitting of electron transitions in the exchange field or due to the spin-orbit interaction. The magnetostrictive birefringence is due to the splitting of electron transitions or degenerate lattice vibrations because of a reduction in the symmetry of the crystal field as a result of magnetostriction.

We can calculate the magnetostrictive birefringence if we know the magnetostriction constants λ_{ijkl}, orientation of the spontaneous magnetization in a crystal, i.e., the direction cosines α_k and α_l, and the piezooptic coefficients.

The piezooptic effect is also observed when a crystal is deformed by an external compressive or tensile force.

This effect can be allowed for in the usual way using Eq. (67). However, an important feature of magnetically ordered crystals is that, because of the magnetoelastic interaction, elastic stresses alter the orientation of the spontaneous magnetization. This means that, in addition to the usual piezooptic effect, we should observe a change in the birefringence because of a change in the orientation of the magnetization. This change affects both the intrinsic magnetic birefringence and the birefringence due to magnetostriction. In practice, the various mechanisms can be separated by applying external forces along the principal crystallographic directions.

VI. INVESTIGATIONS OF MAGNETIC BIREFRINGENCE IN FERROMAGNETS AND ANTIFERROMAGNETS

1. Divalent-europium compounds. The strongest, in the absolute sense, magnetooptic phenomena have been observed so far in divalent-europium compounds such as EuX, where X = O, S, Se, and Te. Magnetic, electrical, and optical properties of europium compounds are discussed in detail in several monographs.[47-50] These compounds have the NaCl-type fcc structure. Crystals of EuO and EuS are typical ferromagnets. Antiferromagnetic order is found in EuSe but even weak fields of 0.1 kOe give rise to a considerable net magnetization and in fields above 8 kOe the magnetic moments are oriented along the field. Antiferromagnetic order is also found in EuTe.

Europium compounds have two strong optical absorption maxima at energies of 2.0–2.5 eV and 4.0–4.7 eV. When the lattice parameter increases, i.e., when the crystal field decreases, the first maximum shifts toward higher energies and the second toward lower energies. This behavior makes it possible to attribute these maxima to the allowed electron transitions $4f^7 \rightarrow 4f^6 5d(t_{2g})$ and $4f^7 \rightarrow 4f^6 5d(e_g)$, respectively. These absorption maxima have a structure which cannot be resolved, even at low temperatures. The structure is most probably due to the spin-orbit splitting of the t_{2g} and e_g states and, at low temperatures, it may also be due to the exchange splitting. A much better resolution of the band structure can be obtained in the magnetic circular and linear dichroism and birefringence spectra. The absorption maxima exhibit an anomalous red shift of the order of 1000–2000 cm^{-1} when a crystal is magnetically ordered.[10,51] The large magnitude of this shift indicates that it is associated with an excited state because the exchange splitting of the ground 4f state should not exceed ~ 100 cm^{-1}.

Dispersion effects, like the circular and linear birefringence, are of considerable interest in the transparency regions of crystals, particularly in the near-infrared and partly in the visible range. The magnetic linear birefringence of europium oxide EuO at T = 20°K in a field of 9 kOe is $n_\perp - n_\parallel = 1.07 \times 10^{-2}$ at a wavelength $\lambda = 10.6\mu$.[52,53] It gradually increases with energy, reaching 1.5×10^{-2} at $\lambda = 2.5\,\mu$. The magnetic linear birefringence of EuSe is also large near the first absorption maximum lying in the red part of the spectrum. The value of this birefringence extrapolated to saturation is $n_\perp - n_\parallel \approx 2.0 \times 10^{-2}$ for $\lambda = 0.725\,\mu$ at T = 4.2°K.[10] This magnetic linear birefringence is the highest ever value recorded for crystals.

The magnetic circular and linear birefringence effects in europium compounds are a consequence of considerable circular and linear dichroism in the regions of the absorption bands, as investigated for crystals of EuO,[52,53] EuS,[54] and EuSe.[10,55]

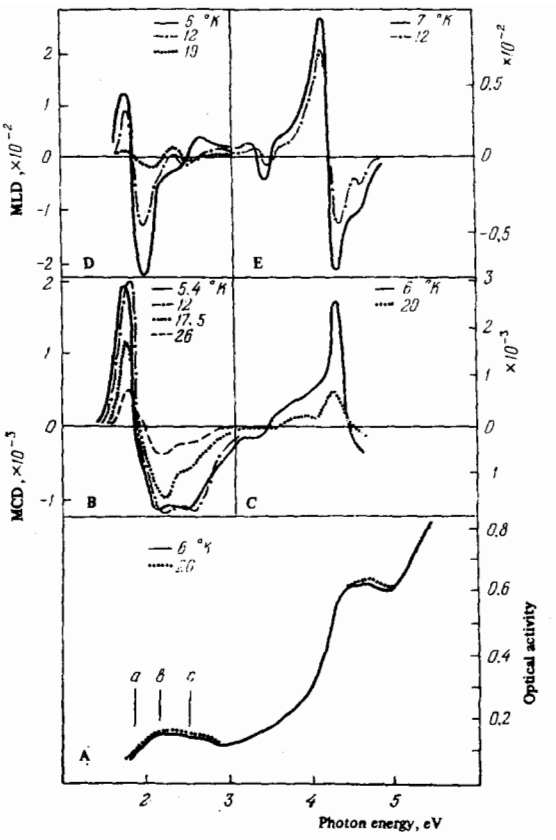

FIG. 3. Absorption spectrum of EuS (A), magnetic circular dichroism (MCD) spectra (B, C), and magnetic linear dichroism (MLD) spectra (D, E) in the vicinity of and below T_C. The dichroism was measured in the following magnetic fields (kOe): B) 0.17; C) 1.4; D) 7.2; E) 0.44 [54].

We shall now consider the main features of these phenomena in the case of EuS.[54] Investigations of the optical absorption and magnetic dichroism were carried out on thin films of this compound deposited in vacuum on polished CaF_2 substrates. The quality of these films was checked by carrying out x-ray structure analysis and verifying that the absorption spectrum and Curie temperature $T_C = 18 \pm 1$°K agreed with the published results. The absorption and dichroism spectra obtained at low temperatures for this compound are plotted in Fig. 3. The structure of the two wide bands is not resolved in the absorption spectra but it is quite clear in the magnetic circular and linear dichroism (MCD and MLD) spectra. The model of a free Eu^{2+} ion can be used to calculate the signs of the MCD (++−) and MLD (+−+) effects for the spin-orbit components (expanded in terms of rising J) of the excited state $^8P_J 4f^6 5d(e_g \text{ or } t_{2g})$. The intermediate state does not appear in the MCD spectrum because of the mutual overlap of two components which have the same sign (++) but it can be clearly distinguished in the MLD spectrum, where the neighboring components have opposite signs. At low temperature, the influence of the exchange interaction varies with the wavelength. For example, it has little influence on the MCD spectrum of bands a and b, but large changes are observed in the region of band c (2.2–3.0 eV). It has not yet been possible to interpret unambiguously the shoulder found in the region of the first absorption band. One of

TABLE III. Comparison of magnitudes and signs of Faraday effect Δn_F and Cotton-Mouton effect Δn_{CM} predicted theoretically and found experimentally [10]

	Theory			Experiment
	$J'=\frac{9}{2}$	$J'=\frac{7}{2}$	$J'=\frac{5}{2}$	
Δn_F	+	−	−	−
Δn_{CM}	−	+	−	−
$\Delta n_{CM}/\Delta n_\Phi$ (20 kOe, 15 °K)	−0.026	−0.26	+0.043	+0.023
$\Delta n_{CM}/\Delta n_\Phi$ (∞, 0 °K)	−0.3	−3	+0.5	−

TABLE IV. Magnetic birefringence of light in iron garnets (T = 295°K, λ = 1.15 μ, and H = 20 kOe)

Crystal	a	H ∥ [100]		H ∥ [111]		Crystal	a	H ∥ [100]		H ∥ [111]	
		$\Delta n_{CM}\cdot 10^5$	β_{CM}, deg/cm	$\Delta n_{CM}\cdot 10^5$	β_{CM}, deg/cm			$\Delta n_{CM}\cdot 10^5$	β_{CM}, deg/cm	$\Delta n_{CM}\cdot 10^5$	β_{CM}, deg/cm
$Y_3Fe_5O_{12}$	1.34	3.87	120	5.16	160	$Dy_3Fe_5O_{12}$	3.67	0.97	30	3.55	110
$Sm_3Fe_5O_{12}$	0.62	8.06	250	5.0	155	$Ho_3Fe_5O_{12}$	1.82	2.72	85	5.00	155
$Eu_3Fe_5O_{12}$	0.98	10.25	320	10.00	312	$Er_3Fe_5O_{12}$	1.52	3.55	110	5.40	167
$Gd_3Fe_5O_{12}$	1.29	4.00	124	5.10	160	$Lu_3Fe_5O_{12}$	1.65	3.20	100	5.30	165
$Tb_3Fe_5O_{12}$	2.67	1.44	45	3.80	115						

the possibilities is the spin-forbidden transition $5d(t_{2g})$ $(S' = 5/2)$, which is mixed with the levels $5d(t_{2g})$ $(S' = 7/2)$ by the spin-orbit or exchange interaction.

Theoretical estimates of the sign and relative magnitude of the Faraday (Δn_F) and Cotton-Mouton (Δn_{CM}) effects based on the intraion transition model are obtained in [10] for paramagnetic europium fluoride EuF_2. The signs of the effects and the ratios $\Delta n_{CM}/\Delta n_F$ obtained for the cases when the main contribution to the effect is due to transitions to the levels of the multiplet $^8P_{J'}(4f^6 5d)$ with $J' = 9/2$, $7/2$, and $5/2$ are listed in Table III. The experiments predict a negative sign for Δn_F and for Δn_{CM}, i.e., the experimental values are in good agreement with the estimates obtained for the case when the lowest level is $^8P_{5/2}$.

2. Iron garnets. Historically, investigations of the magnetooptic phenomena in ferrites were started using crystals with garnet structure. Yttrium and rare-earth iron garnets have the general formula $R_3Fe_5O_{12}$ (R = Y or rare-earth ion). Their structure is described by the cubic space group O_h^{10}-Ia3d and the unit cell contains eight "molecules" (formula units). The garnet structure is such that considerable variations in respect of composition are possible due to replacements of the original ions at tetrahedral, octahedral, and dodecahedral positions.

The first visual observation of the magnetic birefringence of light in iron garnets was reported in [9] and this phenomenon was later studied in [18,56,57]. A general phenomenological discussion of the optical behavior of cubic crystals is given in Sec. 2 of Chap. V. Table IV gives the results of measurements of the magnetic birefringence of garnets carried out with the magnetization oriented along the fourfold and threefold axes and with light traveling at right-angles to the magnetization. At room temperature, the magnetooptic anisotropy a allows us to divide these garnets into two groups: $a < 1$ for samarium and europium garnets and $a > 1$ in all other cases.

Even in the case of yttrium iron garnet, in which the trivalent iron ions occupying the tetrahedral and octahedral positions are only in the S state, the magnetooptic anisotropy is considerable at room temperature

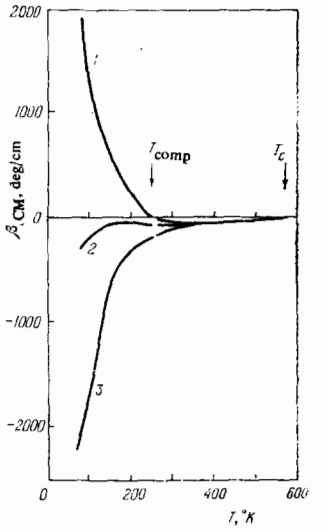

FIG. 4. Temperature dependences of the magnetic birefringence of terbium iron garnet obtained for the magnetization oriented along the [100], [110], and [111] axes (curves 1–3, respectively). The curves represent average experimental results; T_c is the Curie point; T_{comp} is the magnetization compensation temperature; λ = 1.15 μ; H = 23 kOe.

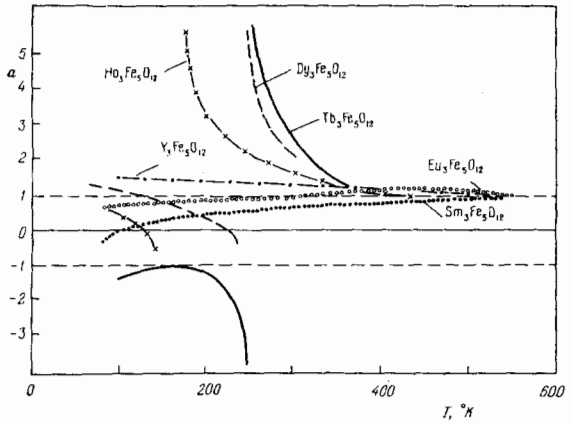

FIG. 5. Temperature dependences of the magnetooptic anisotropy parameter of several rare-earth iron garnets.

(a = 1.3). It is interesting to note that the corresponding ratio for the elastic constants of $Y_3Fe_5O_{12}$ is 0.95, i.e., this crystal is elastically isotropic[58] to within 5%. According to the static measurements,[59] the corresponding ratio of the photoelastic constant is 1.54, whereas it follows from 300 MHz measurements[60] that the ratio is 0.84. The strong anisotropy of the magnetic birefringence shows that its magnitude depends not only on the exchange interaction, whose contribution should be isotropic, but also on anisotropic interactions such as the spin-orbit coupling.

The magnetic birefringence of these garnets, governed by the magnetizations of the iron and rare-earth sublattices, depends very strongly on temperature. Measurements reported in [18,56] extended from 77°K to the Curie temperatures $T_c \sim 550$–580°K. The changes in the birefringence of rare-earth iron garnets are particularly large when the temperature is lowered because there is a change in the order in the rare-earth sublattice. The contribution of this sublattice is large and strongly anisotropic. Figure 4 shows, by way of example, the temperature dependence of the birefringence of terbium iron garnet. When the temperature is increased to the Curie point, the contribution of the rare-earth sublattice decreases: the birefringence curves of the yttrium and rare-earth garnets approach each other.

Figure 5 shows the temperature dependences of the

magnetooptic anisotropy parameter a. Some crystals exhibit anomalies of this parameter near the magnetic compensation points. On approach to the Curie point, the parameter tends to unity for all the investigated garnets. A reasonable explanation of this behavior is not yet available.

The temperature dependence of a indicates that the orientations of the optic axes change. For example, in the case of dysprosium garnet, $Dy_3Fe_5O_{12}$, the orientations of the optic axes vary with temperature from the (001) plane to the (110) plane and then to the $(1\bar{1}0)$ plane, finally returning to the (001) plane. Large rotations of the optic axes are also exhibited by holmium and terbium garnets near the compensation temperatures.

It should be noted that the birefringence may be varied not only by cooling or heating but also by altering the concentration of various magnetic ions.

The most detailed results of the magnetic birefringence of garnets are given in [18,56,57]. The values of this birefringence obtained in two different laboratories are in basic agreement but, for some crystals, there are large discrepancies, particularly at room temperature. These may be due to residual crystallographic stresses. Such stresses may be removed by annealing.[61]

Magnetic ordering of ferrites is accompanied by magnetostrictive strains and this may give rise to the lattice birefringence. However, estimates of this birefringence obtained using known values of the photoelastic and magnetostriction constants show that the magnetostrictive birefringence is approximately two orders of magnitude weaker than the magnetooptic effect.[62,63]

We shall also mention measurements of the birefringence of light in some substituted iron garnets.[64,65] Complex compounds of the $(Gd, Tb, Eu)_3Fe_5O_{12}$ type, exhibiting deviations from the cubic structure,[66] are of special interest among the substituted garnets. The rotation of a plate (made of one of these compounds) about the direction of a light beam in a magnetic field directed along the [110] axis shows that the birefringence differs radically from the curves obtained for cubic garnets. In the absence of this field, a strong birefringence is observed which does not disappear even above the Curie temperature. Bismuth-calcium-vanadium garnets, which do not contain rare-earth ions, behave similarly.[67] Investigations of the orientation and temperature dependences make it possible to attribute the observed birefringence to the crystallographic distortions of the cubic structure of the garnet rather than to the magnetostrictive deformation or domain structure.

3. The ferrimagnet $RbNiF_3$. The great majority of crystals of the 3d-metal fluorides are antiferromagnetic and some exhibit a weak moment. The hexagonal structure of $RbNiF_3$ (space group D_{6h}^4) is interesting because it admits the existence of the ferromagnetic, ferrimagnetic, and antiferromagnetic order. The antiferromagnetic order occurs in $CsMnF_3$ (see Sec. 1 in Chap. VIII). The ferrimagnetic order in fluoride crystals was first observed in $RbNiF_3$. Divalent nickel ions occupy two positions, usually denoted by 4f and 2a. Since the number of 4f ions is twice as large as the number of 2a ions and the spins of the 4f and 2a ions are antiparallel, a spontaneous moment appears in the ordered range and, at low temperatures, this moment reaches $\sigma_S = 21$ cgs esu/g,[68] which represents one-third of the expected magnetization for a parallel distribution of spins in both sublattices. The results of static magnetic, resonance, and optical investigations indicate that below $T_C = 139°K$ the sublattice spins lie in a plane perpendicular to the optic (hexagonal) axis, i.e., $RbNiF_3$ is a ferrimagnet of the easy-plane type. When the magnetic field is applied in the basal plane, saturation is observed in fields of the order of 0.2 kOe, and when the magnetization is along the hexagonal axis, such saturation occurs in fields of 20–24 kOe.[69] Since the linear magnetooptic phenomena, such as the Faraday effect and magnetic circular dichroism, can be observed in their pure form only for light traveling along the optic axis, fairly high magnetic fields are needed to observe saturation of these effects.

In studies of the quadratic effects, a light beam is usually directed perpendicular to the magnetization. Therefore, the saturation magnetic birefringence of $RbNiF_3$ due to propagation of light along the hexagonal axis is observed in a weak field of ~0.2 kOe. In this field, the sixfold axis ceases to be the optic axis and the crystal becomes optically biaxial. The birefringence observed in saturation fields at 77°K in the transparency window at $\lambda = 0.55\ \mu$ is 142 deg/cm, whereas the Faraday effect under the same conditions is only 95 deg/cm.[70]

A magnetic birefringence hysteresis, associated with the domain structure,[71] is observed in $RbNiF_3$. In the linear Faraday effect, the direction of rotation of the plane of polarization changes with the direction of the field but the sign of the quadratic effect remains constant. Consequently, the magnetic birefringence hysteresis loop is of a special shape.

Crystals of $RbNiF_3$ are transparent in wide parts of the spectrum in the visible, ultraviolet, and infrared regions. This can be used to measure the dispersion of the Faraday and Cotton-Mouton effects and the magnetic dichroism spectra over a considerable spectral range.[69,71] Figure 6 shows the dispersion of the magnetic birefringence and the absorption spectrum of $RbNiF_3$.

In the investigated parts of the spectrum, the Cotton-Mouton effect is governed by electron transitions in Ni^{2+} ions. The greatest contribution is due to allowed electric-dipole transitions between electronic configurations, $3d^8 \rightarrow 4p3d^7$, and this contribution lies in the far-ultraviolet part of the spectrum. Complex dispersion of the magnetic birefringence is observed in the region of electron transitions within the 3d shell. The nature of the observed dispersion of the Cotton-Mouton effect is different from the dispersion of the Faraday effect and

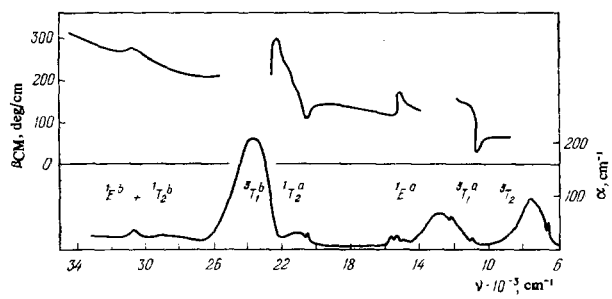

FIG. 6. Dispersion of the magnetic birefringence (upper curve) and absorption spectrum along the hexagonal axis (lower curve) of the ferromagnet $RbNiF_3$ at 77°K.

the contribution of transitions in the 3d shell to the dispersion of the Faraday rotation is greater than in the Cotton-Mouton effect. It should be noted that, in contrast to the quadratic effect, the sign of the Faraday effect changes several times in the spectral range under consideration.[69] For example, several sharp lines are observed in the region of transitions to the $^3T_1^a$ and $^1T_2^a$ levels in the magnetic circular dichroism spectrum but some of them are not observed in the linear dichroism.

An analysis of the magnetic linear dichroism of the $^1E^a$ and $^1T_2^a$ absorption bands, carried out for the ferrimagnet $RbNiF_3$,[71] antiferromagnet $KNiF_3$,[72] and weak ferromagnet NiF_2[73] shows that the sign of this effect is governed by the magnetic structure of the crystal. Special features of the magnetic linear dishroism of the last two antiferromagnets will be considered again in Chap. VII.

The dispersion of the Faraday and Cotton-Mouton effects is usually, even over a narrow part of the spectrum, the sum of the circular and linear dichroisms of the absorption bands throughout the spectral range. This relationship can be established in its general form from the Kramers-Kronig formulas. Hence, it is clear that investigations of the magnetic dichroism of individual transitions may provide information of considerable interest in studies of the microscopic mechanisms responsible for the magnetooptic effects. Unfortunately, very little of such information has been published so far.

VII. INVESTIGATIONS OF MAGNETIC BIREFRINGENCE IN ANTIFERROMAGNETS

1. **Magnetic birefringence in the antiferromagnets α-Fe_2O_3, $RbFeF_3$, $CsMnF_3$, $MnWO_4$, and K_2MnF_4.** The magnetic birefringence of antiferromagnets is associated primarily with the antiferromagnetic vector l, representing the sublattice magnetizations. The birefringence associated with the ferromagnetic vector m has not yet been observed for antiferromagnets because it is considerably smaller. However, this contribution is large in ferromagnetic crystals.

In this section, we shall review briefly investigations of the magnetic birefringence exhibited by certain antiferromagnets with different magnetic structures. Later, we shall discuss in detail the results of studies of the birefringence of fluorides with rutile structure and of transition-metal carbonates.

Hematite (α-Fe_2O_3). This crystal has a structure with the space group D_{3d}^6. Below $T_M \sim 250$–$260°K$, the spins are parallel to the crystal axis and the state is purely antiferromagnetic, whereas, at higher temperatures, the spins lie in the basal plane and are rotated slightly relative to one another, which gives rise to a weak ferromagnetic moment. The symmetry properties of α-Fe_2O_3 are discussed in detail in [27,74].

The magnetic birefringence of hematite was investigated in [75] for light traveling along the optic axis. Figure 7 shows the temperature dependence of the birefringence in the vicinity of the phase transition from the purely antiferromagnetic state to one with a weak moment. Hematite exhibits a considerable absorption in the visible range and the reported measurements were carried out at $\lambda = 1.15\,\mu$.

According to a crystal-optics analysis given in Chap. V for uniaxial crystals of trigonal symmetry, a crystal

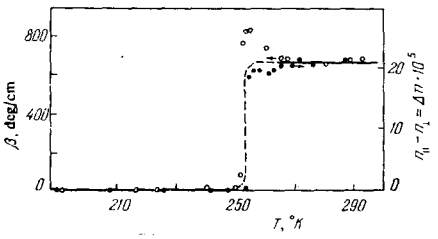

FIG. 7. Temperature dependence of the magnetic birefringence of hematite α-Fe_2O_3 for $\lambda = 1.15\,\mu$ and H = 8 kOe. The effect appears at the Morin point, when the antiferromagnetic moment becomes oriented at right-angles to the direction of propagation of light.

remains uniaxial when the vector l is oriented along the trigonal axis and the birefringence vanishes for the propagation of light along this axis. This is indeed observed experimentally below the Morin point $T_M \approx 253°K$. However, when the vector l deviates from the trigonal axis, we should observe the birefringence described by Eq. (59). It is interesting to note that if the vector l is perpendicular to the trigonal axis, the birefringence is independent of the orientation l in the basal plane. When the vector l deviates from the basal plane, we should observe anisotropy of the birefringence of the order of $2\alpha_3\beta_{14}/(\beta_{11} - \beta_{12})$, where α_3 is the cosine of the angle between l and the trigonal axis, and β_{ik} is the magnetooptic constant.

$CsMnF_3$. The birefringence of this hexagonal antiferromagnet was investigated in [45]. The space group of this crystal is D_{6h}^4 and a unit cell contains two types of site (4f and 2a), occupied by paramagnetic divalent manganese ions. Below the Néel point $T_N = 53.5°K$, this crystal transforms to a magnetically ordered state and the spins are oriented in the basal plane. It follows from symmetry considerations that weak ferromagnetism is impossible in this crystal and $CsMnF_3$ is indeed a "pure" antiferromagnet. It should be noted that the symmetry of this hexagonal crystal allows the existence of the ferromagnetic or ferrimagnetic order. The latter is observed in $RbNiF_3$.

The complex crystal structure of $CsMnF_3$ (and of $RbNiF_3$) makes the magnetooptic phenomena in these crystals dependent on a large number of parameters. For a specific antiferromagnetic order of the spins in the two sublattices of $CsMnF_3$, namely,

$$\begin{aligned} l_1 &= S_1 - S_2, \\ l_2 &= -\sigma_1 + \sigma_2 + \sigma_3 - \sigma_4 \end{aligned} \qquad (69)$$

[where S_i (i = 1, 2) and σ_j (j = 1, 2, 3, 4) are the magnetic moments of the ions in the 2a and 4f lattices], the number of coefficients is nineteen.[45] The expansion employed for this crystal contains only terms quadratic in l and l_2.

Figure 13 (given later in the paper) shows the temperature dependence of the birefringence of $CsMnF_3$ obtained for light traveling at right-angles to the optic axis: $\mathbf{k} \parallel Oy$. This crystal remains optically uniaxial at all temperatures and in all magnetic fields applied in the basal plane (x, y). The value of $\Delta n_{xz}(T)$ varies strongly in the region of T_N. Unfortunately, the purely magnetic contribution to the birefringence cannot be separated for this crystal because the temperature dependences of the lattice constants are not known.

$RbFeF_3$. This crystal is cubic at room temperature (perovskite-type structure) but, at low temperatures, exhibits several phase (magnetic and crystallographic)

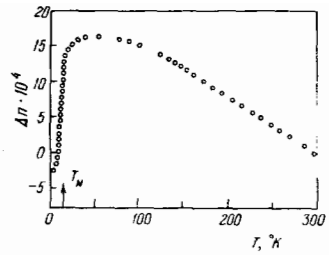

FIG. 8. Temperature dependence of the birefringence of light in $MnWO_4$.

transitions.[76,77] Investigations of the optical absorption have demonstrated that this crystal is transparent in wide regions at infrared, visible, and ultraviolet frequencies.[78,79] The absorption bands in the region of 7020 and 9760 cm^{-1} are due to electron transitions $^5T_{2g} \rightarrow {}^5E_g$ in the Fe^{2+} ions acted upon by an octahedral crystal field. At higher frequencies, there are weaker absorption maxima due to electron transitions in the Fe^{2+} ions accompanied by a change in spin.

The paramagnetic birefringence is exhibited by this crystal at 200°K. In the transparency range at ν = 18,000 cm^{-1}, it amounts to $\Delta n \approx 10^{-6}$ in a field of ~30 kOe. This effect varies quadratically with the field. The birefringence at 77°K (orthorhombic phase with a spontaneous magnetic moment) was measured in the plane of one of the principal sections of the refractive index ellipsoid. In this case, the effect is $\Delta n \approx 2 \times 10^{-4}$ in weak fields and a strong differential rise is observed when the field is increased. This suggests that, at 77°K, $RbFeF_3$ has a noncollinear (canted) magnetic structure.[80]

At 82°K, the birefringence of $RbFeF_3$ is 9×10^{-5} at 4000 Å and 1.6×10^{-4} at 8000 Å in a 5 kOe field.[78]

$MnWO_4$. Measurements of the crystallographic and magnetic birefringence are reported for this crystal in [81]. The crystal is monoclinic and its space group is P2/c. The refractive-index ellipsoid is oriented so that Ox ∥ b, Oy ∥ a, and the z axis is oriented at an angle of 17–21° with respect to the c axis (for red light produced by a lithium lamp). The angle between the optic axes is $2V_z$ = 75° and the crystal is optically positive. The room-temperature refractive indices are n_x = 2.17 ± 0.01, n_y = 2.22 ± 0.01, and n_z = 2.32 ± 0.01.

A study of the birefringence was carried out on a plate of the (010) type and, in this case, the room-temperature birefringence was found to be $n_z - n_y = 0.1$. The temperature dependence of the birefringence is plotted in Fig. 8. In the magnetic ordering region ($T_N \approx 15$°K), there is a clear contribution of the magnetic birefringence, $\sim 2 \times 10^{-3}$, but a detailed separation of the crystallographic and magnetic contributions has yet to be made.

K_2MnF_4. This compound has the tetragonal D_{4h}^{17} structure. Paramagnetic ions form layers perpendicular to the fourfold axis in which the exchange interaction is stronger than between the layers. Below T_N = 42.1°K, K_2MnF_4 assumes full antiferromagnetic order and, at higher temperatures in the vicinity of T_N, the short-range order in the layers predominates so that the crystal is a "two-dimensional" antiferromagnet.

The birefringence of light in K_2MnF_4 was investigated in [82]. A large magnetic contribution was found not only in the antiferromagnetic state but also above T_N right up to 200°K, i.e., up to ~5T_N. The temperature dependence of the magnetic birefringence of K_2MnF_4 differs considerably from the behavior of a three-dimensional antiferromagnet. In the latter case, the contribution of the short-range order is relatively weak compared with the effect in the ordered region and the derivative $d(\Delta n)/dT$ has a sharp extremum in the region of T_N, which coincides with the position of the maximum in the specific heat curve.

In layered structures, such as K_2MnF_4, the dominant contribution is due to the short-range order and the $d(\Delta n)/dT$ curve has a wide rounded maximum above T_N, which is typical of the temperature dependence of the specific heat of two-dimensional systems.

2. Birefringence of light in rutile antiferromagnets. Detailed measurements of the magnetic and crystallographic birefringence have been carried out on antiferromagnets with the rutile structure.[46,81] This class of crystals is interesting because they have relatively simple crystallographic and magnetic structures and many of their crystallographic and physical properties are known in sufficient detail.

These crystals are tetragonal and the space group is D_{4h}^{14}. In the paramagnetic range of temperature, they are optically uniaxial and the natural crystallographic birefringence is $n_e - n_0 \sim 10^{-2}$, as reported in [81] (Table V).

The antiferromagnetic vector **l** of manganese, iron, and cobalt fluorides is directed along the [001] fourfold axis. Below the Néel temperature, nickel fluoride goes over to a state with a weak ferromagnetic moment **m** in a plane perpendicular to the fourfold axis and directed along the [100] or [010] axis. The vector **l** lies in the same plane and is perpendicular to **m**.[83] Some of the properties of crystals with the rutile structure are listed in Table V. The values of T_N are deduced from the temperature dependence of the specific heat,[84] the magnetic properties are taken from [46], and the refractive indices at 300°K for λ = 6328 Å are taken from [81].

The birefringence was investigated in [46,81] for light traveling at right-angles and parallel to the tetragonal axis. Figure 9 shows the temperature dependences of the birefringence for $\mathbf{k} \perp [001]$ at λ = 6328 Å obtained for several fluorides with rutile structure. The bire-

TABLE V. Some optical and magnetic properties of crystals with rutile structure

Compound	T_N, °K	H_E, kOe	H_D, kOe	$\chi_\perp \cdot 10^3$, cgs esu/mole	n_e	n_0
MnF_2	67.5	500	—	24.5	1.4992	1.4706
FeF_2	78.35	—	—	—	1.5213	1.5113
CoF_2	37.70	770	241	55	1.5331	1.5069
NiF_2	73.22	1430	28	6	1.5562	1.5212

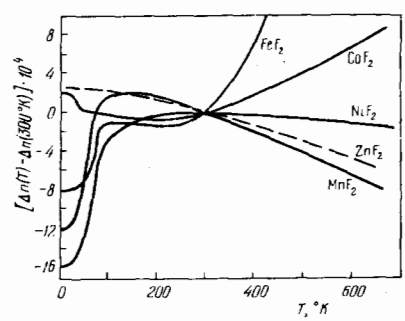

FIG. 9. Temperature dependences of the birefringence of light in crystals with the rutile structure. [81] For clarity, the room-temperature birefringence of all crystals is assumed to be zero.

fringence varies strongly near the magnetic ordering temperature and the changes in this region should be attributed to the magnetic contribution. In the paramagnetic region far from T_N, the variation of the birefringence should be attributed to changes in the lattice constants. Thus, the observed changes include the magnetic and lattice contributions:

$$\Delta n\,(T) = \Delta n_M\,(T) - \Delta n_{\text{latt}}\,(T). \qquad (70)$$

The lattice contribution itself is due to the change in the birefringence resulting from the usual thermal expansion Δn_{th} and changes associated with the spontaneous magnetostriction Δn_{str}.

At high temperatures, far from T_N, the relationship between the observed change in the birefringence $\Delta n(T)$ and the change in the lattice parameters can be represented by the linear dependence

$$\frac{d}{dT}\,[\Delta n(T)] = k[\beta_c(T) - \beta_a(T)], \qquad (71)$$

where β_c and β_a are the linear expansion coefficients along the c and a axes in the tetragonal lattice. Since between 0 and 700°K the changes in the lattice constants amount to a few percent, the value of k can be assumed to be independent of temperature. In fact, investigations of the birefringence indicate that this quantity can be regarded as constant for a given crystal and this is true of paramagnetic (MnF_2, FeF_2, CoF_2) and diamagnetic (MgF_2, ZnF_2) fluorides. The constant k should vary from crystal to crystal and depend on the frequency of light. Thus, if we know k, we can use the measurements carried out at high temperatures when the magnetic contribution is negligible, to calculate $\Delta n_{latt}(T)$ at low temperatures and the difference between the measured and lattice birefringence gives the pure magnetic contribution.

This contribution was separated for all the investigated fluorides with the rutile structure. At low temperatures, Δn_M was found to be of the order of $(1-2)\times 10^{-3}$. A comparison of the dependence $\Delta n_M(T)$ with the dependence of the square of the sublattice magnetization l^2 indicated that $\Delta n_M(T)$ did not vary as rapidly as the former (Fig. 10). This indicates that below T_N we have $\overline{l^2} - \overline{l}^2 \neq 0$, i.e., there are considerable fluctuations in the vector l. In the case of MnF_2 at 2–60°K, this difference

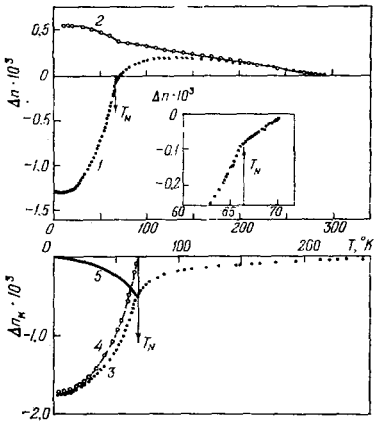

FIG. 10. Temperature dependences of the birefringence of light in MnF_2: [46] 1–experimental dependences; 2–dependence calculated using the contribution represented by Eq. (70); 3–magnetic birefringence deduced from curve 1 by subtracting curve 2; 4–temperature dependence of the square of the static sublattice magnetization, deduced from NMR experiments; 5–difference between curves 3 and 4.

can be approximated by the law αT^2. It is pointed out in [46] that this law is not a trivial consequence of the spin-wave theory because the latter is valid only at temperatures $T \ll T_N$.

The dependence $\Delta n(T)$ has a kink at the Néel temperature (see the inset in Fig. 10), which agrees well with the position of the maximum in the specific heat curve. It follows from general considerations that the observed value of Δn_M is proportional to the magnetic energy of a crystal, i.e.,

$$\frac{d\,[\Delta n_M\,(T)]}{dT} \propto c_M,$$

where c_M is the magnetic specific heat. A detailed comparison shows that this relationship is satisfied very well over a wide temperature range (Fig. 11). The magnetic contribution to the birefringence does not disappear directly at T_N but is retained to temperatures of $\sim(2-3)T_N$ because of the short-range magnetic order. It should be noted that this short-range order may play a role also in noncubic crystals when light travels at right-angles to a selected direction. In cubic crystals or in the case of propagation of light along the optic axis of a uniaxial crystal, the short-range order should not affect the birefringence. The value of Δn_M obtained for uniaxial crystals in the isotropic state is proportional to the mean value of the square of the total antiferromagnetic moment. Consequently, the mean value $\overline{\Delta(\Delta n_M)}$ due to deviations of the vector l from its static value, does not vanish. The main contribution to the birefringence is due to fluctuations in l whose typical lifetimes are two or three orders of magnitude greater than the period of oscillations of the light wave and whose characteristic dimensions are considerably smaller than the wavelength of light $a \ll \lambda$. The variation of Δn_M in the temperature range 70–110°K can be approximated [46] by the dependence

$$\Delta n_M \propto T^{-2,7}. \qquad (72)$$

We have seen in Chap. V that Eq. (62), for the density of the internal electromagnetic energy, including terms which are quadratic in respect of the components of the

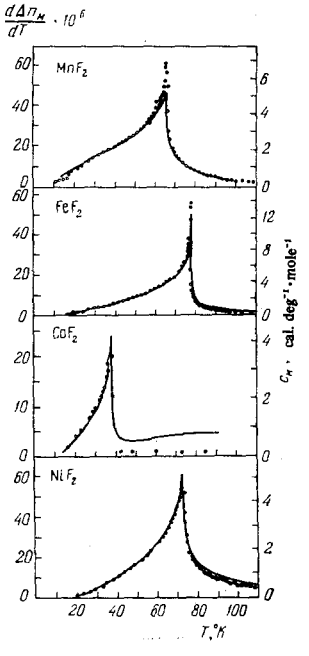

FIG. 11. Comparison of the temperature dependences of the derivative of the magnetic birefringence $d\Delta n_M/dT$ (circles) and of the magnetic specific heat c_M (continuous curves) of several antiferromagnets. [81]

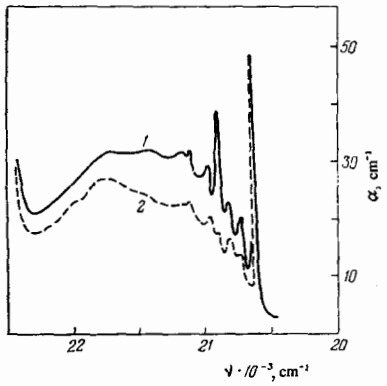

FIG. 12. Magnetic linear dichroism of the $^3A_2 \rightarrow {}^1T_2^3$ transition in Ni^{2+} ions in NiF_2 for T = 1.8°K and H = 1 kOe. The absorption coefficients are given for polarized light: 1) $\alpha_{E\parallel M}$; 2) $\alpha_{E\parallel M}$. [73]

antiferromagnetic vector, allows us to separate the isotropic and anisotropic contributions to the magnetic birefringence. Such separation has been carried out for MnF_2, CoF_2, and NiF_2 crystals by varying the orientation of the vector l in a crystal subjected to an external magnetic field. No changes in the birefringence are observed for MnF_2 and NiF_2 and hence it is concluded that the birefringence is independent of the orientation of the vector l relative to the crystallographic axes, i.e., the anisotropic corrections to the permittivity are small compared with the isotropic contribution. In the case of CoF_2, the birefringence changes when the vector l is rotated, i.e., the anisotropic corrections are significant against a background of the isotropic contribution.

The absence of anisotropic terms in the case of MnF_2 means that the crystal remains optically uniaxial for any orientation of the vector l. In the case of NiF_2, for which the vector l is in the basal plane, the anisotropic terms give rise to biaxial optical properties.[81] It is found that the new optic axes deviate slightly from the tetragonal axis of the crystal. The angle between the optic axes is $2V_Z \approx 2°$ at 30°K. Significant biaxial properties are also exhibited by CoF_2.

Apart from the birefringence of NiF_2, a study was also made of the linear dichroism of this crystal.[73] A considerable crystallographic dichroism was observed for many electron transitions in the Ni^{2+} ion when light was polarized parallel and perpendicular to the optic axis. However, it was fairly difficult to separate the magnetic contribution in this geometry. It was possible to do this for the propagation of light parallel to the optic axis. Figure 12 shows the results of an investigation of NiF_2 in the region of one of the electron transitions. The absorption coefficients $\alpha_{E\parallel M}$ and $\alpha_{E\perp M}$ differ after the orientation of the antiferromagnetic domains by an external field and the difference between these coefficients gives the magnetic linear dichroism. An explanation of this effect is given in [73] on the basis of the spin-orbit interaction, which makes the probability of electron transitions vary with the polarization of incident light.

3. Antiferromagnetic manganese and cobalt carbonates. The birefringence of light in manganese and cobalt carbonates was investigated in [44,45]. These crystals belong to the D_{3d} class of the trigonal system and the crystallographic symmetry has the space group D_{3d}^6 in the paramagnetic region. A unit cell of these carbonates contains two magnetic ions. When the temperature is lowered, these crystals assume magnetically

TABLE VI. Some magnetic and optical properties of manganese and cobalt carbonates [45]

Compound	T_N, °K		H_E, kOe	H_D, kOe	$\chi_\perp \cdot 10^3$, cgs esu/mole	n_0 (T=300 °K)	n_e (T=300 °K)
$MnCO_3$	29.5	32.4	320	4.4	43	1.816	1.597
$CoCO_3$	17.0	18.1	160	27	52	1.855	1.60

ordered states (Table VI) of the easy-plane type. The magnetic vectors of the sublattices in these carbonates are inclined and give rise to a spontaneous ferromagnetic vector σ which lies in the basal plane and is perpendicular to the antiferromganetic vector l. Some magnetic and optical properties of these carbonates are given in Table VI.

Figure 13 gives the temperature dependences of the birefringence of these carbonates for light traveling along the y axis, i.e., at right-angles to the optic axis of the crystals. An important change in the nature of the temperature dependence of Δn_{XZ} is observed near the Néel point. Clearly, the insufficient precision of the measurements has destroyed the kink in the curve Δn(T) at the Néel point of $MnCO_3$. Nevertheless, at 32°K, there is a maximum of the derivative $d(\Delta n_{XZ})/dT$, which agrees well with the results of magnetic measurements (32.4°K) but differs from 29.5°K deduced from the specific heat. The value of Δn_{XZ} of $MnCO_3$ is not affected by the application of a magnetic field up to 50 kOe in the basal plane H ∥ Ox. Moreover, no changes are observed in the other configuration in which light is propagated parallel to the z axis. The difference $\Delta n_{XY}(T) = n_X - n_Y$ vanishes in all fields and at all temperatures. It follows from these experiments that the magnetic birefringence of $MnCO_3$, like that of MnF_2, is independent of the orientation of the vector l, relative to the crystallographic axes.

A kink is observed in the curve $\Delta n_{XZ}(T)$ obtained for $CoCO_3$ recorded with and without the field at 17°K. This value is in good agreement with the Néel point deduced from the specific heat measurements. Moreover, the birefringence of $CoCO_3$ depends on the orientation of the vector l relative to the crystallographic axes. This anisotropic contribution is observed for light traveling perpendicular and parallel to the optic axis.

The potential usefulness of the magnetic birefringence as a method for studies of domains in rhombohedral antiferromagnets with a weak ferromagnetic moment was investigated in [44] in the specific case of cobalt carbonate in the visible part of the spectrum by the conoscopic figure method. The acute angle 2V between the optic axes was determined for a crystal magnetized to saturation. Light traveled along the trigonal axis. Knowing the refractive indices for the ordinary and extraordinary rays in the paramagnetic region made it possible to determine the magnetic birefringence along the bisector of the acute angle 2V using Eq. (61). Figure 14 shows the temperature dependence of this acute angle 2V. According to Eq. (61), the value of 2V should be a linear function of the antiferromagnetic vector l. It is clear from Fig. 14 that the results of the optical measurements are in good agreement with the value of the spontaneous ferromagnetic moment m (which is proportional to l). At low temperatures, the acute angle in question is about 3°, i.e., the optic axes deviate only slightly from the trigonal axis of the crystal.

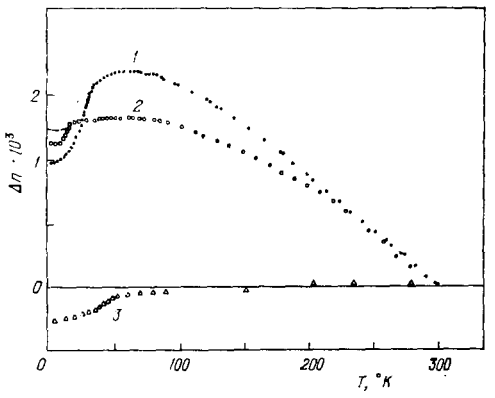

FIG. 13. Temperature dependences of the difference between the refractive indices of the ordinary and extraordinary rays $\Delta n = n_{\perp} - n_{\parallel}$ plotted for $MnCO_3$ (1), $CoCO_3$ (2), and $CsMnF_3$ (3). Below T_N in $CoCO_3$, the circles denote the dependence of Δn in a magnetic field of 2 kOe and the dashed curve is the dependence in the absence of the magnetic field. [45]

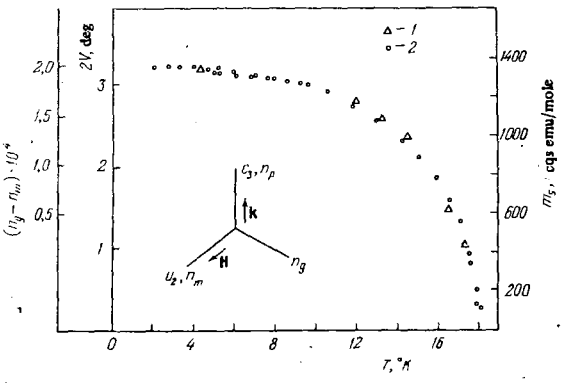

FIG. 14. Temperature dependences of the acute angle 2V between the optic axes, of the birefringence of light $n_g - n_m$, and of the spontaneous ferromagnetic moment m_s. [44]

VIII. CONCLUSIONS

Recent investigations have established the basic ideas about the magnetic linear birefringence of a large group of crystals with different types of magnetic order (ferromagnetic, ferrimagnetic, and antiferromagnetic). A phenomenological theory of the magnetooptic phenomena in these crystals is based on the principles of magnetic symmetry. The heuristicity of this method is confirmed by the prediction of several new magnetooptic phenomena, many of which have not yet been investigated. The next step should be the development of a microscopic theory of these phenomena and experimental investigations.

In contrast to the diamagnets and paramagnets, magnetically ordered media exhibit a strong linear magnetic birefringence Δn which may reach 10^{-2}–10^{-4} and is explained by the exchange interactions. The large value of this effect is also frequently accompanied by a strong magnetooptic anisotropy.

This review deals with some aspects of the crystal optics of magnetically ordered media, which require further studies to establish more rigorously the nature of the interaction of light with these crystals. Some characteristic crystal-optics phenomena arise from the coexistence of comparable linear and quadratic magnetic birefringence effects.

An important point is the establishment of the correlations between the magnetooptic properties and other characteristics of magnetic crystals. In some cases, one can only speak of a qualitative correspondence between the temperature dependences of the sublattice magnetizations and magnetic linear birefringence (rare-earth iron garnets), whereas in other cases a good quantitative correspondence has been established between the birefringence and specific heat (fluorides with the rutile structure).

Most of the investigations have been carried out so far at fixed wavelengths and the number of investigations of wider spectral ranges is small. Nevertheless, studies of the magnetic dichroism in the electron transition region may provide a reliable experimental basis for theoretical calculations.

The large magnitudes of the magnetic linear birefringence and dichroism in magnetically ordered crystals and the high sensitivity of modern methods for recording the polarization of light and its changes may result in extensive applications of these effects in studies of magnetic crystals.

The same properties of magnetic crystals and the possibility of changing them by external agencies, in combination with a fairly high optical transparency, should make these materials useful in various technical applications.

[1] J. W. Beams Jr, Rev. Mod. Phys. 4, 133 (1932).
[2] G. Szivessy, Handbuch der Physik, Vol. 21, Springer Verlag, Berlin, 1929, p. 823.
[3] J. Becquerel, Radium (Paris) 4, 49 (1907); 5, 5 (1908); 6, 327 (1909); Commun. Phys. Lab. Univ. Leiden 189, No. 68a, 127 (1929).
[4] J. F. Dillon Jr, J. Appl. Phys. 39, 922 (1968).
[5] G. S. Krinchik and M. V. Chetkin, Usp. Fiz. Nauk 98, 3 (1969) [Sov. Phys.-Usp. 12, 307 (1969)].
[6] N. F. Kharchenko and V. V. Eremenko, Fiz. Kondens. Sost. (Kharkov) No. 4, 144 (1969); No. 13, 3 (1971).
[7] N. V. Starostin and P. P. Feofilov, Usp. Fiz. Nauk 97, 621 (1969) [Sov. Phys.-Usp. 12, 252 (1969)].
[8] J. F. Dillon Jr, in: Magnetic Properties of Materials (ed. J. Smit), McGraw-Hill, New York, 1971, Chap. 5.
[9] J. F. Dillon Jr, J. Appl. Phys. 29, 1286 (1958).
[10] J. C. Suits, B. E. Argyle, and M. J. Freiser, J. Appl. Phys. 37, 1396 (1966).
[11] L. D. Landau and E. M. Lifshitz, Élektrodinamika sploshnykh sred, Gostekhizdat, M., 1957 (Electrodynamics of Continuous Media, Pergamon Press, Oxford, 1960).
[12] W. J. Tabor and F. S. Chen, J. Appl. Phys. 40, 2760 (1969).
[13] W. A. Shurcliff, Polarized Light: Production and Use, Harvard University Press, Cambridge, Mass., 1962 (Russ. Transl., Mir, M., 1965).
[14] R. V. Pisarev, I. G. Siniĭ, and G. A. Smolenskiĭ, Izv. Akad. Nauk SSSR Ser. Fiz. 34, 1032 (1970)].
[15] V. D. Tron'ko, Opt. Spektrosk. 29, 354 (1970) [Opt. Spectrosc. 29, 187 (1970)].
[16] B. Desormiere and H. le Gall, Solid State Commun. 9, 1029 (1971).
[17] F. V. Lisovskiĭ, Opt. Spektrosk. 34, 947 (1973) [Opt. Spectrosc. 34, 545 (1973)].
[18] R. V. Pisarev, I. G. Siniĭ, N. N. Kolpakova, and Yu. M. Yakovlev, Zh. Eksp. Teor. Fiz. 60, 2188 (1971) [Sov. Phys.-JETP 33, 1175 (1971)].
[19] F. I. Fedorov, Optika anizotropnykh sred (Optics of

Anisotropic Media), Izd. AN BSSR, Minsk, 1958.
[20]M. I. Kaganov and R. P. Yankelevich, Fiz. Tverd. Tela 10, 2771 (1968) [Sov. Phys.-Solid State 10, 2181 (1969)].
[21]R. R. Birss and R. G. Shrubsall. Philos. Mag. 15, 687 (1967).
[22]T. H. O'Dell, Philos. Mag. 7, 1653 (1962); 8. 411 (1963).
[23]R. Fuchs, Philos. Mag. 11, 647 (1965).
[24]V. N. Lyubimov, Kristallografiya 14, 213 (1969) [Sov. Phys.-Crystallogr. 14, 168 (1969)].
[25]D. N. Astrov, Zh. Eksp. Teor. Fiz. 38, 984 (1960) [Sov. Phys.-JETP 11, 708 (1960)].
[26]R. M. Hornreich and S. Shtrikman, Phys. Rev. 171, 1065 (1968).
[27]I. E. Dzyaloshinskiĭ, Zh. Eksp. Teor. Fiz. 32, 1547 (1957) [Sov. Phys.-JETP 5, 1259 (1957)].
[28]A. S. Borovik-Romanov, Zh. Eksp. Teor. Fiz. 36, 766 (1959) [Sov. Phys.-JETP 9, 539 (1959)]; A. S. Borovik-Romanov and V. I. Ozhogin, Zh. Eksp. Teor. Fiz. 39, 27 (1960) [Sov. Phys.-JETP 12, 18 (1961)].
[29]A. S. Borovik-Romanov, Zh. Eksp. Teor. Fiz. 36, 1954 (1959) [Sov. Phys.-JETP 9, 1390 (1959)]; 38, 1088 (1960) [11, 786 (1960)].
[30]E. A. Turov and V. G. Shavrov, Zh. Eksp. Teor. Fiz. 43, 2273 (1962) [Sov. Phys.-JETP 16, 1606 (1963)]; Izv. Akad. Nauk SSSR Ser. Fiz. 27, 1487 (1963).
[31]R. V. Pisarev, Zh. Eksp. Teor. Fiz. 58, 1421 (1970) [Sov. Phys.-JETP 31, 761 (1970)].
[32]S. Bhagavantam, Proc. Indian Acad. Sci. A73, 269 (1971).
[33]R. R. Birss, Symmetry and Magnetism, North-Holland, Amsterdam, 1964.
[34]V. M. Agranovich and V. L. Ginzburg, Kristallooptika s uchetom prostranstvennoĭ dispersii i teoriya éksitonov, Nauka M., 1965 (Spatial Dispersion in Crystal Optics and the Theory of Excitons, Wiley, New York, 1967).
[35]T. Moriya, J. Phys. Soc. Jap. 23, 490 (1967); J. Appl. Phys. 39, 1042 (1968).
[36]Y. R. Shen and N. Bloembergen, Phys. Rev. 133, A515 (1964).
[37]H. le Gall, J. Phys. (Paris) 32, Suppl. C1, 590 (1971).
[38]H. R. Hulme, Proc. R. Soc. A135, 237 (1932).
[39]S. V. Vonsovskiĭ and A. V. Sokolov, Zh. Eksp. Teor. Fiz. 19, 703 (1949).
[40]P. N. Argyres, Phys. Rev. 97, 334 (1955).
[41]A. M. Clogston, J. Phys. Radium 20, 151 (1959); J. Appl. Phys. Suppl. 31, 198S (1960).
[42]J. F. Dillon Jr, H. Kamimura, and J. P. Remeika, J. Phys. Chem. Solids 27, 1531 (1966).
[43]J. F. Nye, Physical Properties of Crystals, Clarendon Press, Oxford, 1957 (Russ. Transl., Mir, M., 1967).
[44]N. F. Kharchenko, V. V. Eremenko, and O. P. Tutakina, Zh. Eksp. Teor. Fiz. 64, 1326 (1973) [Sov. Phys.-JETP 37, 672 (1973)].
[45]A. S. Borovik-Romanov, N. M. Kreĭnes, and M. A. Talalaev, ZhETF Pis'ma Red. 13, 80 (1971) [JETP Lett. 13, 54 (1971)]; A. S. Borovik-Romanov, I. M. Kreĭnes, A. A. Pankov, and M. A. Talalaev, Zh. Eksp. Teor. Fiz. 66, 782 (1974) [Sov. Phys.-JETP 39, 378 (1974)].
[46]A. S. Borovik-Romanov, I. M. Kreĭnes, A. A. Pankov, and M. A. Talalaev, Zh. Eksp. Teor. Fiz. 64, 1762 (1973) [Sov. Phys.-JETP 37, 890 (1973)].
[47]S. Methfessel and D. C. Mattis, "Magnetic semiconductors," in: Handbuch der Physik, Vol. 18, Part 1, Springer Verlag, Berlin, 1968, pp. 389-562 (Russ. Transl., Mir, M., 1972).
[48]C. Haas, IEEE Trans. Magn. MAG-5, 487 (1969).
[49]I. G. Austin and D. Elwell, Contemp. Phys. 11, 455 (1970).
[50]CRC Crit. Rev. Solid State Sci. (July 1972).
[51]G. Busch. and P. Wachter, Phys. Kondens. Mater. 5, 232 (1966).
[52]J. O. Dimmock, C. E. Hurwitz, and T. B. Reed, Appl. Phys. Lett. 14, 49 (1969).
[53]J. O. Dimmock, C. E. Hurwitz, and T. B. Reed, J. Appl. Phys. 40, 1336 (1969).
[54]J. Ferre, B. Briat, C. Paparoditis. S. Pokrzywnicki, and R. Suryanaryanan, Solid State Commun. 11, 1173 (1972).
[55]B. E. Argyle, J. C. Suits, and M. J. Freiser, Phys. Rev. Lett. 15, 822 (1965).
[56]G. A. Smolenskiĭ, R. V. Pisarev, I. G. Siniĭ, N. N. Kolpakova, and A. G. Titova, Izv. Akad. Nauk SSSR Ser. Fiz. 36, 1219 (1972).
[57]J. F. Dillon Jr, J. P. Remeika, and C. R. Staton, J. Appl. Phys. 41, 4613 (1970).
[58]A. E. Clark and R. E. Strakna, J. Appl. Phys. 32, 1172 (1961).
[59]R. T. Lynch Jr, J. E. Dillon Jr, and L. G. Van Uitert, J. Appl. Phys. 44, 225 (1973).
[60]R. W. Dixon, J. Appl. Phys. 38, 5149 (1967).
[61]V. A. Babko and V. D. Tron'ko, Fiz. Tverd. Tela 14, 2795 (1972) [Sov. Phys.-Solid State 14, 2426 (1973)].
[62]R. V. Pisarev, I. G. Siniĭ, and G. A. Smolenskiĭ, Fiz. Tverd. Tela 12, 118 (1970) [Sov. Phys.-Solid State 12, 93 (1970)].
[63]L. M. Dedukh and V. I. Nikitenko, Fiz. Tverd. Tela 12, 1768 (1970) [Sov. Phys.-Solid State 12, 1400 (1970)].
[64]J. F. Dillon Jr, E. M. Georgy, and J. P. Remeika, AIP Conf. Proc. 5, 190 (1971).
[65]R. V. Pisarev, N. N. Kolpakova, Yu. M. Yakovlev, V. S. Filonich, and A. G. Titova, Fiz. Tverd. Tela 14, 360 (1972)] [Sov. Phys.-Solid State 14, 300 (1972)].
[66]A. N. Bobeck, E. G. Spencer, L. G. Van Uitert, S. C. Abrahams, R. L. Barns, W. H. Grodkiewicz, R. C. Sherwood, P. H. Schmidt, D. H. Smith, and E. M. Walters, Appl. Phys. Lett. 17, 131 (1970).
[67]N. N. Kolpakova, R. V. Pisarev, M. Zh. Eganyan, and Yu. M. Yakovlev, Fiz. Tverd. Tela 16, 1999 (1974) [Sov. Phys.-Solid State 16, 1300 (1975)].
[68]M. W. Shafer, T. R. McGuire, B. E. Argyle, and G. T. Fan, Appl. Phys. Lett. 10, 202 (1967).
[69]R. V. Pisarev, I. G. Siniĭ, and G. A. Smolenskiĭ, Fiz. Tverd. Tela 9, 3149 (1967) [Sov. Phys.-Solid State 9, 2482 (1968)].
[70]R. V. Pisarev, I. G. Siniĭ, and G. A. Smolenskiĭ, ZhETF Pis'ma Red. 9, 112 (1969) [JETP Lett. 9, 64 (1969)].
[71]I. G. Siniĭ and R. V. Pisarev, Fiz. Tverd. Tela 12, 114 (1970) [Sov. Phys.-Solid State 12, 89 (1970)].
[72]R. V. Pisarev, J. Ferre, J. Duran, and J. Badoz, Solid State Commun. 11, 913 (1972).
[73]P. Moch and M. Balkansky, in: Optical Properties of Ions in Crystals (Proc. Conf. John Hopkins University, Baltimore, Md., 1966), Interscience, New York, 1967; P. Moch, Thèse, Paris 1967.
[74]A. S. Borovik-Romanov, Itogi nauki: Fiz.-matem. nauki (Progress in Science: Physicomathematical Sciences), Vol. 4, VINITI, M., 1962.
[75]R. V. Pisarev, I. G. Siniĭ, and G. A. Smolenskiĭ, ZhETF Pis'ma Red. 9, 294 (1969) [JETP Lett. 9, 172 (1969)].
[76]L. R. Testardi, H. J. Levinstein, and H. J. Guggenheim, Phys. Rev. Lett. 19, 503 (1967).
[77]G. K. Wertheim, H. J. Guggenheim, H. J. Williams, and D. N. E. Buchanan, Phys. Rev. 158, 446 (1967).
[78]F. S. Chen, H. J. Guggenheim, H. J. Levinstein, and S. Singh, Phys. Rev. Lett. 19, 948 (1967).

[79]R. V. Pisarev, V. V. Druzhinin, N. N. Nesterova, S. D. Prokhorova (Prochorova), and G. T. Andreeva, Phys. Status Solidi **40**, 503 (1970).
[80]I. G. Siniĭ, R. V. Pisarev, P. P. Syrnikov, G. A. Smolenskiĭ, and A. I. Kapustin, Fiz. Tverd. Tela **10**, 2252 (1968) [Sov. Phys.-Solid State **10**, 1775 (1969)].
[81]I. R. Jahn and H. Dachs, Solid State Commun. **9**, 1617 (1971); I. R. Jahn, Dissertation, Institut für Kristallographie der Universität Tübingen, 1971; Phys. Status Solidi b **57**, 681 (1973).
[82]I. R. Jahn and W. Jauch, in: Proc. International Conference on Magnetism, Moscow, 1973, Vol. 2, Nauka, Moscow, 1974, p. 103.
[83]R. A. Alikhanov, Zh. Eksp. Teor. Fiz. **37**, 1145 (1959) [Sov. Phys.-JETP **10**, 814 (1960)].
[84]J. W. Stout and E. Catalano, J. Chem. Phys. **23**, 2013 (1955).

Translated by A. Tybulewicz